Defense Threat Reduction Agency
8725 John J. Kingman Road, MS-6201
Fort Belvoir, VA 22060-6201

DTRA-TR-15-023

TECHNICAL REPORT

Updates to Blast Injury Criteria Models for Nuclear Casualty Estimation

DISTRIBUTION A. Approved for public release: distribution is unlimited.

December 2015

HDTRA1-14-D-0003; 0005

Prepared by:

Nuclear Survivability and Forensics
Integrated Program Team

REPORT DOCUMENTATION PAGE

Form Approved
OMB No. 0704-0188

Public reporting burden for this collection of information is estimated to average 1 hour per response, including the time for reviewing instructions, searching existing data sources, gathering and maintaining the data needed, and completing and reviewing this collection of information. Send comments regarding this burden estimate or any other aspect of this collection of information, including suggestions for reducing this burden to Department of Defense, Washington Headquarters Services, Directorate for Information Operations and Reports (0704-0188), 1215 Jefferson Davis Highway, Suite 1204, Arlington, VA 22202-4302. Respondents should be aware that notwithstanding any other provision of law, no person shall be subject to any penalty for failing to comply with a collection of information if it does not display a currently valid OMB control number. **PLEASE DO NOT RETURN YOUR FORM TO THE ABOVE ADDRESS.**

1. REPORT DATE *(DD-MM-YYYY)*	**2. REPORT TYPE**	**3. DATES COVERED** *(From - To)*
00-12-2015	Technical	

4. TITLE AND SUBTITLE

Updates to Blast Injury Criteria Models for Nuclear Casualty Estimation

5a. CONTRACT NUMBER
HDTRA1-14-D-0003

5b. GRANT NUMBER

5c. PROGRAM ELEMENT NUMBER

6. AUTHOR(S)

Jacqueline Wentz
Daniela Stricklin
Kyle Millage

5d. PROJECT NUMBER

5e. TASK NUMBER
0005

5f. WORK UNIT NUMBER

7. PERFORMING ORGANIZATION NAME(S) AND ADDRESS(ES)

Applied Research Associates, Inc.
801 N. Quincy Street, Suite 700
Arlington, VA 22203

8. PERFORMING ORGANIZATION REPORT NUMBER

DTRA-TR-15-023

9. SPONSORING / MONITORING AGENCY NAME(S) AND ADDRESS(ES)

Nuclear Technologies Directorate
Defense Threat Reduction Agency
8725 John J. Kingman Road, Mail Stop 6201
Fort Belvoir, VA 22060-6201

10. SPONSOR/MONITOR'S ACRONYM(S)

DTRA

11. SPONSOR/MONITOR'S REPORT NUMBER(S)

DTRA-TR-15-23

12. DISTRIBUTION / AVAILABILITY STATEMENT

Distribution Statement A. Approved for public release; distribution is unlimited.

13. SUPPLEMENTARY NOTES

14. ABSTRACT

This report recommends blast injury criteria models to be implemented in our Health Effects from Nuclear and Radiation Environments software platform. Calculating blast injury probability is a two-step process where, first, the velocity of the human body or missile is determined and, second, this velocity is related to the likelihood of injury using probit models. We review and critique existing methodologies used by nuclear effects communities. Based on this review, we propose adjustments to minimize uncertainties and allow injury criteria to be calculated in urban environments. Probit models for tertiary injury (i.e., decelerative tumbling and perpendicular impact) and secondary injury (i.e., stone/glass penetration and blunt trauma) are presented. For each injury type, multiple injury levels exist ranging from moderate to fatal.

15. SUBJECT TERMS

Blast Injury, Nuclear Casualty, HENRE, Translation Model, Injury Probit Model

16. SECURITY CLASSIFICATION OF:			**17. LIMITATION OF ABSTRACT**	**18. NUMBER OF PAGES**	**19a. NAME OF RESPONSIBLE PERSON**
a. REPORT	**b. ABSTRACT**	**c. THIS PAGE**			Paul K. Blake, PhD
Unclassified	Unclassified	Unclassified	UU	66	**19b. TELEPHONE NUMBER** *(include area code)* 703-767-3433

UNIT CONVERSION TABLE

U.S. customary units to and from international units of measurement*

U.S. Customary Units	Multiply by → / ← Divide by†		International Units
Length/Area/Volume			
inch (in)	2.54	$\times 10^{-2}$	meter (m)
foot (ft)	3.048	$\times 10^{-1}$	meter (m)
yard (yd)	9.144	$\times 10^{-1}$	meter (m)
mile (mi, international)	1.609 344	$\times 10^{3}$	meter (m)
mile (nmi, nautical, U.S.)	1.852	$\times 10^{3}$	meter (m)
barn (b)	1	$\times 10^{-28}$	square meter (m^2)
gallon (gal, U.S. liquid)	3.785 412	$\times 10^{-3}$	cubic meter (m^3)
cubic foot (ft^3)	2.831 685	$\times 10^{-2}$	cubic meter (m^3)
Mass/Density			
pound (lb)	4.535 924	$\times 10^{-1}$	kilogram (kg)
atomic mass unit (AMU)	1.660 539	$\times 10^{-27}$	kilogram (kg)
pound-mass per cubic foot (lb ft^{-3})	1.601 846	$\times 10^{1}$	kilogram per cubic meter (kg m^{-3})
Pound-force (lbf avoirdupois)	4.448 222		Newton (N)
Energy/Work/Power			
electron volt (eV)	1.602 177	$\times 10^{-19}$	joule (J)
erg	1	$\times 10^{-7}$	joule (J)
kiloton (kT) (TNT equivalent)	4.184	$\times 10^{12}$	joule (J)
British thermal unit (Btu) (thermochemical)	1.054 350	$\times 10^{3}$	joule (J)
foot-pound-force (ft lbf)	1.355 818		joule (J)
calorie (cal) (thermochemical)	4.184		joule (J)
Pressure			
atmosphere (atm)	1.013 250	$\times 10^{5}$	pascal (Pa)
pound force per square inch (psi)	6.984 757	$\times 10^{3}$	pascal (Pa)
Temperature			
degree Fahrenheit (^oF)	$[T(^oF) - 32]/1.8$		degree Celsius (^oC)
degree Fahrenheit (^oF)	$[T(^oF) + 459.67]/1.8$		kelvin (K)

*Specific details regarding the implementation of SI units may be viewed at http://www.bipm.org/en/si/.

†Multiply the U.S. customary unit by the factor to get the international unit. Divide the international unit by the factor to get the U.S. customary unit.

Table of Contents

List of Figures

List of Tables

Acknowledgements

The authors gratefully acknowledge the support provided by:

- Dr. Paul Blake of DTRA/J9 for programmatic support.
- LTC Andrew Scott and Matthew Jackson of U.S. Army Nuclear and Chemical Weapons of Mass Destruction Agency for their support in answering questions related to this work.
- Dr. Charles Needham for his expertise in blast effects.

Executive Summary

This report reviews current approaches and provides adjusted methodologies for predicting the probability of blast-related injuries following nuclear detonations in both urban and open field environments. The purpose of this research is to integrate the optimal models into our Health Effects of Nuclear and Radiological Environments platform which is a suite of physiological models that predicts health effects in nuclear and radiological environments. The blast injury criteria models predict the likelihood of tertiary and secondary injuries based on blast wave and object parameters. Separate models are used for different injury levels, including moderate, serious, and fatal categories.

Current approaches for predicting the likelihood of blast-related injury use a two-step process. First, the maximum velocity obtained by the human body or secondary missile is determined through the interpolation of values in look-up tables. These tables provide velocity as a function of peak overpressure and yield. Next, probit models are used to predict the probability of secondary or tertiary injury as a function of the object's velocity. We sought to review both these steps and, if needed, adjust the methodologies to predict injury in urban environments. The traditional method to determine an object's velocity used by the nuclear effects communities assumes a specific blast wave shape. However, in urban environments, complex overpressure and dynamic pressure waveforms are likely. Thus, rather than using the peak overpressure and yield to calculate velocity, we propose the use of a translation model that uses physical principles to relate an object's acceleration to the dynamic pressure and wind velocity as a function of time. For the next step of the process (i.e., relating velocity to injury), we review existing probit models used by nuclear effects communities. This review includes a detailed analysis of source data, assumptions, and ambiguities in each probit model generation. In several cases where the models were based on limited data, included unrealistic assumptions, and/or large ambiguities existed, we developed new criteria models using contemporary data. Finally, based on our review we recommend models to be included in our Health Effects of Nuclear and Radiological Environments platform.

1 Introduction

Applied Research Associates, Inc. (ARA) has been tasked by the Defense Threat Reduction Agency (DTRA) to support their mission to safeguard against weapons of mass destruction. A subtask of this project involves implementing models that predict the probability of mortality and injury following nuclear detonations in urban environments. This report reviews current approaches for estimating blast-related casualties and, where appropriate, recommends alternate methodologies. The optimal approaches will be selected for integration into our Health Effects of Nuclear and Radiological Environments (HENRE) platform which is a suite of physiological models that predict prompt and protracted health effects of nuclear and radiological environments. Ultimately, HENRE models will be integrated into other tools such as NucFast or DTRA's Hazard Prediction and Assessment Capability (HPAC) tool to improve current casualty estimation capabilities and better account for urban environments, combined injuries, and the time-course of effects. Both HPAC and NucFast provide location and time-specific blast wave parameters that can serve as input to the blast injury criteria models. Therefore, based on the reliability of the underlying data, we identify the most suitable blast injury criteria models for implementation into HENRE and subsequent integration into HPAC or NucFast.

The three categories of blast injury are primary, secondary, and tertiary. Primary injuries are caused by the direct effects of the blast wave overpressure on the human body. Secondary injuries are caused by missiles that are accelerated by the blast wave. Tertiary injuries are caused by the acceleration of the human body and the ensuing deceleration. In this work, we focus on secondary and tertiary injuries. Because of the dramatic effects experienced from blast, thermal, and radiation interactions associated with nuclear detonations, persons experiencing primary blast injuries will also encounter other lethal exposures. Therefore, for our purposes, we exclude an analysis of primary blast injuries.

Calculating the probability of secondary or tertiary injury due to blast is a two-step process: (1) human or missile velocities are determined based on blast wave parameters and (2) probit models relate the velocity of an object to the probability of injury. The Personnel Risk and Casualty Criteria (PRCC) report and Effects Manual-1 Chapter 14 (EM-1 Ch. 14) provide starting points for this endeavor (Department of the Army 2013; Drake et al. 1993; Reeves 2015). Both of these documents use look-up tables developed in the 1970s to determine the velocity of a human or missile based on peak overpressure and yield (Fletcher et al. 1975). Next, probit models are used to relate object velocity to the likelihood of injury.

Based on known shortcomings and a review of the literature, we identified two near-term issues that could be addressed to more accurately predict blast-related injuries in urban environments:

1. Velocity Calculations: Current approaches use peak overpressure and yield to predict injury, but this is not an accurate method when considering the complex waveforms that occur in urban environments. We suggest a revised approach in which a translation model developed by Lovelace Foundation for Medical Education and Research (LFMER) is used to predict the velocity of objects based on the incident-specific blast wave parameters (see Section 3).

2. Injury Calculations: The existing probits relating velocity to injury are based on limited data (Section 4 provides a review of these probit models and the corresponding source data). Due to the many assumptions involved in the generation of the existing probit models, where possible, we propose new probit models that integrate more contemporary data.

The combined translation and probit models provide improvements to probability of injury predictions for complex blast wave scenarios.

2 Methods

To select models for integration into HENRE 2.0, we reviewed current approaches for estimating injury and mortality due to nuclear blast. In reviewing existing methodologies, we focused on approaches currently used by the nuclear effects communities. It is possible that relevant models used by other communities exist; however, these are not reviewed here. Sources reviewed include EM-1 Ch. 14 (Drake et al. 1993; Reeves 2015), the PRCC 2013 report (Department of the Army 2013), the Allied Medical Publication 8 (AmedP-8) North Atlantic Treaty Organization (NATO) planning guide (NATO 2009), and methodologies present by Dr. John Mercier at the Human Response Panel (HRP) in the early 2000s (Mercier 2001). The models presented by Dr. Mercier are used within the Probability of Damage Calculator (PDCALC), a tool used by HPAC to estimate human injury in nuclear environments (Jackson et al. 2013). In reviewing existing models, our goal was to select the optimal models for inclusion in HENRE 2.0. Thus, we sought to fully understand the derivation and accuracy of existing models.

While reviewing the existing probit models used to relate velocity to injury, several issues arose. In some cases, the data used to develop the models were not obtainable or not referenced and, thus, could not be reviewed. In other cases, when the data was available, the existing probit could not be derived. Finally, in several cases, potentially unrealistic assumptions were used to generate the probit models.

When these issues arose, we sought, if feasible, to generate new probit models by either re-deriving the probit using the original data or creating a new probit using contemporary data. In some cases, we developed more general probit equations. For example, multiple penetration probits exist for missiles of different masses. Instead of using these probits, we developed probits which include both mass and velocity in the probit equation.

All computational procedures were performed in R v3.1.2 (R Core Team 2014). Translation simulations were performed using the general solver for ordinary different equations from the deSolve library (Soetaert et al. 2010b). Least-square regression was performed using the modCost and modFit tools from the Flexible Modeling Environment (FME) Library (Soetaert et al. 2010a). Probit models were fit to data using generalized linear models (Venables et al. 2002). R code for running the translation model and generating the output data and plots given in Section 3 is provided in Appendix A.

3 Translation Model

In the 1960s, LFMER developed a translation model which predicts the acceleration, velocity and translation distance of objects exposed to a blast wave based on attributes of the object, including mass and orientation (Bowen et al. 1961). An updated version of this model takes into account deceleration due to ground friction (Fletcher et al. 1966). Using these models, LFMER performed a series of simulations to develop look-up tables for different initial orientations which relate the maximum velocity of a human to blast wave parameters (Fletcher et al. 1975). These tables are referenced today by both the 2013 PRCC report and EM-1 Ch. 14 as the source for blast injury criteria (Drake et al. 1993; Reeves 2015; Department of the Army 2013). Through the interpolation of the values in these tables, velocity is calculated as a function of peak overpressure and yield. The approach used in the 2013 PRCC report and EM-1 Ch. 14 assumes the blast waveforms of interest have the same shape and duration as the ones originally used to generate the look-up tables.

In this section, we discuss an alternate approach for calculating an object's velocity. To provide the probability of injury after exposure to a complex blast wave, rather than using look-up tables, we have implemented the original translation model developed by LFMER (Bowen et al. 1961; Fletcher et al. 1966). The maximum velocity of an object is calculated using the time-dependent overpressure, dynamic pressure, wind velocity, and shock wave velocity. This method eliminates assumptions about the shape and duration of the blast wave that are inherent when using the look-up tables. While this approach requires additional time-dependent environment inputs leading to longer computing times, it also improves accuracy by more precisely calculating the maximum velocity for a given scenario. This section describes our implementation of the translation model, as well as the verification and validation of the model.

In developing the translation model, we assume the direction of the dynamic pressure and wind velocity is constant. However, due to the complex nature of urban environments this may not be the case. Later versions of the model should use vector notation to predict how changes in wind and dynamic pressure direction would affect translation.

3.1 Translation Model Nomenclature

In developing the translation model, we use a terminology similar to Bowen et al. 1961. Dimensional quantities are represented with a lowercase letter (except for temperature). The dimensionless quantity is either represented with the corresponding uppercase character or, if unavailable, with a tilde. The parameters used to make quantities dimensionless do not change during the blast scenario.

Time:

t = time after blast wave arrival
t_p^+ = duration of positive overpressure
t_u^+ = duration of positive winds
$\widetilde{t}_p = t/t_p^+$
$\widetilde{t}_u = t/t_u^+$

Velocity:

c_0 = speed of sound in undisturbed air
u = wind velocity
$\dot{x}$ = shock wave velocity
v = velocity of the moving object
$U = u/c_0$
$\dot{X} = \dot{x}/c_0$
$V = v/c_0$

Pressure:

p_0 = ambient pressure
p = overpressure
q = dyanmic pressure
$P = p/p_0$
$Q = q/p_0$

Distance:

d = distance traveled by object
$D = d/(c_0 t_u^+)$

Object Parameters:

m = mass of object
s = area of object presented to the wind
C_d = drag coefficient of object
$\alpha = sC_d/m$ (acceleration coefficient)
m_0 = average mass of human; 75 kg (165 lb)
$A = \alpha p_0 t_u^+/c_0$
$M = m/m_0$

Air Temperature:

T = temperature
T_0 = ambient temperature
$\widetilde{T} = T/T_0$

Air Density:

ρ = air density
R = gas constant of air
$\widetilde{\rho} = \rho R T_0/P_0$

Note that an s subscript refers to the value of that variable at the shock front. For example, p_s is the overpressure at the shock front.

3.2 Object Acceleration

This section presents our implementation and verification of the translation model developed by Bowen et al. 1961. This model describes an object's translation profile (i.e., acceleration, velocity, and distance traveled) over time following a blast wave exposure. Appendix A.2 gives the R function that was used to run the model. For small debris, this model is sufficient; however, for larger objects, such as animals and humans, the incorporation of deceleration is essential and will be described in Section 3.3.

3.2.1 Model Implementation

The following equation gives the time-dependent acceleration of a generic object exposed to a blast wave (Bowen et al. 1961)

$$\frac{dv}{dt} = q\alpha \left(\frac{u - v}{u} \right)^2 \tag{1}$$

where v is the object's velocity, q is the dynamic pressure, and u is the wind velocity. Note that q and u are the values at the location of the object, and this location changes as the object moves through space. The acceleration coefficient α is specific to the object of interest, taking into account attributes such as surface area exposed to the blast wave, shape, and mass (see Section 3.1, Nomenclature). This equation was derived by equating the drag force of the blast wave winds with the force needed to cause object acceleration.

A dimensionless form of Equation 1, given by Bowen et al. 1961, can be written as follows with the appropriate substitutions (see Section 3.1, Nomenclature):

$$\frac{dV}{d\widetilde{t}_u} = QA \left(\frac{U - V}{U} \right)^2 \tag{2}$$

Equation 2 defines the acceleration portion of the translation model that will be used to predict the maximum velocity an object obtains.

3.2.2 Model Verification

To verify that the acceleration model (Equation 2) correctly matches the original version of the model (Bowen et al. 1961), we used the blast wave parameters specified in the report as the inputs and compared the resulting outputs.

The time profile for the dimensionless dynamic pressure at a point in space is defined as (Bowen et al. 1961)

$$Q = Q_s(1 - \widetilde{t}_u)(Je^{-\gamma \widetilde{t}_u} + Ke^{-\delta \widetilde{t}_u}) \tag{3}$$

where

$$Q_s = \frac{2.5P_s^2}{7 + P_s} \frac{1 + 2 \cdot 10^{-8} P_s^4}{1 + 10^{-8} P_s^4} \tag{4}$$

$$J = \begin{cases} 1.186 P_s^{1/3} & \text{if } P_s < 0.6 \\ 1 & \text{if } 0.6 \leq P_s \leq 1.0 \\ \frac{10^4 P_s^{-1/4}}{10^4 + P_s^2} & \text{if } P_s > 1.0 \end{cases} \tag{5}$$

$$K = 1 - J \tag{6}$$
$$\gamma = 1/4 + 3.6P_s^{1/2} \tag{7}$$
$$\delta = 7 + 8P_s^{1/2} + 2P_s^2/(240 + P_s). \tag{8}$$

The time profile for the dimensionless wind velocity at a point in space is

$$U = U_s(1 - \widetilde{t}_u)e^{-\nu\widetilde{t}_u} \tag{9}$$

where

$$U_s = P_s/(1 + P_s^{1/2}) \tag{10}$$
$$\nu = P_s^{1/3} + 0.0032P_s^{3/2}. \tag{11}$$

Equations 2–11 define the blast wave parameters at a constant point in space. To run model simulations, we are interested in the blast wave parameters at the location of the object. To make this transformation we change $\widetilde{t}_u$ in Equations 3 and 9 to

$$\widetilde{t}_u - \frac{D}{\dot{X}_s} \tag{12}$$

where $\dot{X}_s$ represents the dimensionless speed of the shock wave propagation and D represents the dimensionless distance traveled by the object at time $\widetilde{t}_u$. Equation 12 represents the amount of time since the shock wave front was at D, rather than the amount of time since the shock wave front was at the object's starting position. This transformation assumes that any decay due to radial expansion of the shock wave is negligible.

The dimensionless velocity of the pressure propagation $\dot{X}$ is related to the dimensionless wind velocity U according to the following Equation[1]:

$$\dot{X}_s = \frac{3}{5}U_s + \sqrt{1 + \left(\frac{3}{5}U_s\right)^2} \tag{13}$$

The resulting simulations agree with outputs tabulated in the report (Figure 3.1). For all simulations shown in Figure 3.1, $P_s = 0.10$. Simulations were stopped when the object's velocity was equal to the wind velocity at the location of the object.

In a second verification to dimensional output given by Bowen et al. 1961, the parameters in Table 3.1 were used. The relationship between t_u^+ and t_p^+ was determined through the digitization of Figure 2.2 from Bowen et al. 1961. Based on these parameters, a maximum velocity of 7.01 m/s (23.0 ft/s) was obtained which is very close to the value given in the report of 7.13 m/s (23.4 ft/s).

Based on these verification results, we are satisfied that the acceleration model is accurately reproduced here. The slight discrepancies between the model and the data that exist are likely caused by errors in digitization and different numerical procedures.

[1]This equation was derived by Bowen et al. 1961 from Shapiro 1954 (Pg 1001, Equation 25.20) by setting u_1 to zero, u_2/c_1 to U, W/c_1 to $\dot{X}$, and k to 1.4.

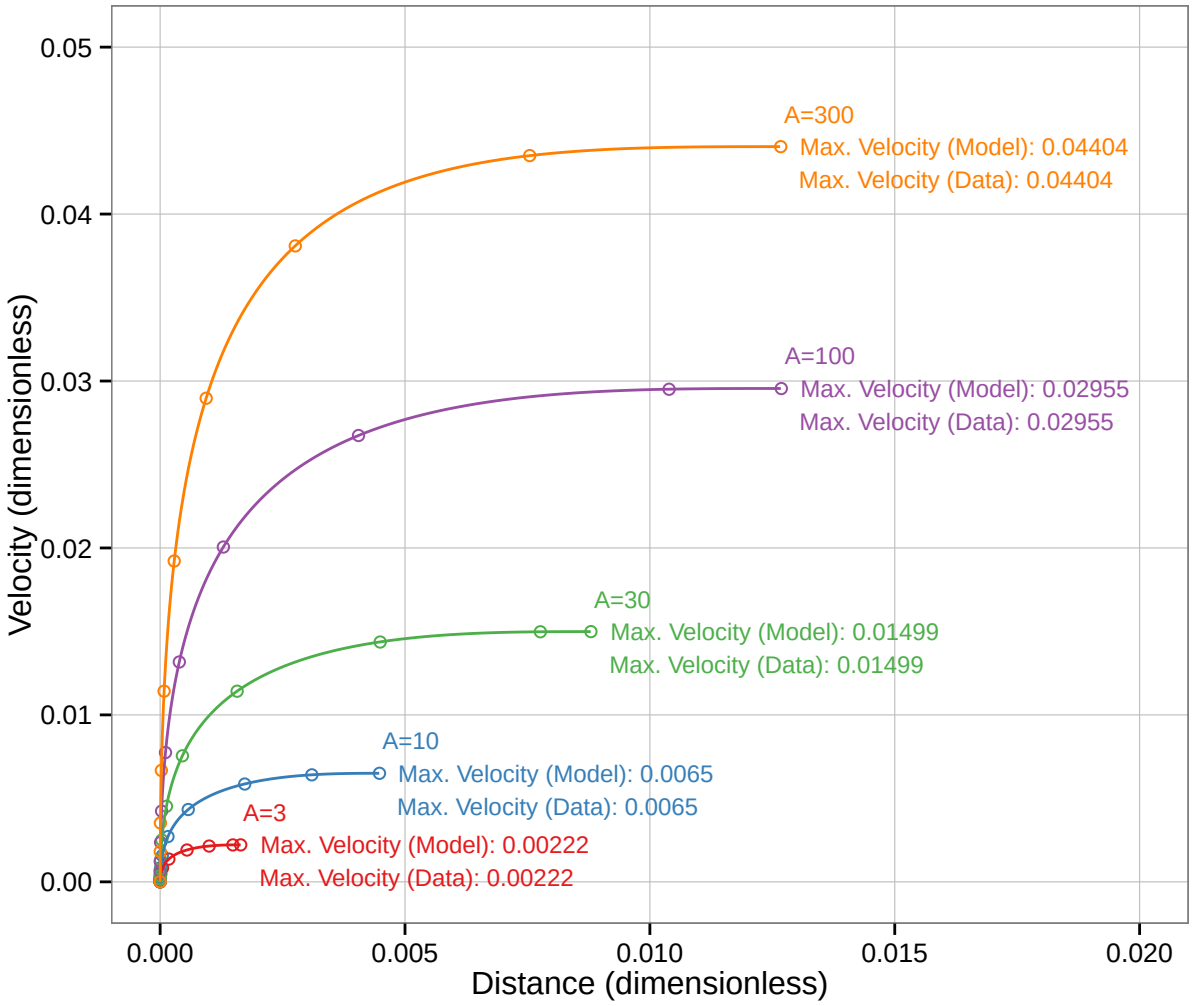

Figure 3.1: Verification of the acceleration model implementation. Data digitized from Bowen et al. 1961, Table 4.1.

Table 3.1: Parameters used for dimensional acceleration model verification.

Parameter	Value
α	0.0061 m^2/kg (0.03 ft^2/lb)
p_s	36.5 kPa (5.3 psi)
p_0	91.7 kPa (13.3 psi)
t_p^+	0.964 s
t_u^+	1.216 s*
c_0	341.4 m/s (1120 ft/s)

*Value was obtained through the digitization of Figure 2.2 from Bowen et al. 1961.

3.3 Object Deceleration

This section describes the implementation and verification of the decelerative portion of the translation model that was developed by LFMER (Fletcher et al. 1966). The deceleration rate was quantified by LFMER using experimental animal data with initial speeds ranging from 4.47 to 26.82 m/s. The stopping distance was determined as a function of the initial velocity and the mass of the animal. This empirical relationship was in turn used to determine the deceleration rate.

3.3.1 Model Implementation

The relationship between velocity and stopping distance is

$$\log_{10}\left(x\left(\frac{m_0}{m}\right)^{1/3}\right) = -a + b\log_{10}\left(v\left(\frac{m_0}{m}\right)^{1/6}\right) \tag{14}$$

where x is the distance traveled before stopping, m is the weight of the animal, m_0 is the average weight of a man or 75 kg (165 lbs), and v is the initial velocity. Using Equation 14, the instantaneous deceleration is given as[2]

$$\frac{dv}{dt} = -F\left(v\left(\frac{m_0}{m}\right)^{1/6}\right)^B \tag{20}$$

where $F = 4.278\ \mathrm{m}^{1-B}\mathrm{s}^{B-2}$ and $B = 0.38308$.

The deceleration term given by Equation 20 is made dimensionless using the appropriate substitutions (see Section 3.1, Nomenclature) and is incorporated into the translation model

[2] Equation 14 implies that the distance traveled over the time interval $[t_0,t_{end}]$ is

$$x(t_{end}) - x(t_0) = 10^{-a}\cdot\left(\frac{m_0}{m}\right)^{b/6-1/3} v(t_0)^b. \tag{15}$$

We assume this relationship holds for all $t \in [t_0, t_{end}]$. That is , we assume the distance "remaining" at time t (i.e., the distance traveled over the time interval $[t,t_{end}]$) is

$$x(t_{end}) - x(t) = 10^{-a}\cdot\left(\frac{m_0}{m}\right)^{b/6-1/3} v(t)^b. \tag{16}$$

Therefore,

$$\int_t^{t_{end}} v(s)ds = 10^{-a}\cdot\left(\frac{m_0}{m}\right)^{b/6-1/3} v(t)^b. \tag{17}$$

Differentiating Equation 17 with respect to t, we obtain

$$-v(t) = 10^{-a}\cdot\left(\frac{m_0}{m}\right)^{b/6-1/3} bv(t)^{b-1}\frac{dv}{dt} \tag{18}$$

and solve for deceleration

$$\frac{dv}{dt} = -\frac{1}{b\cdot 10^{-a}}\left(v\left(\frac{m_0}{m}\right)^{1/6}\right)^{2-b}. \tag{19}$$

Equation 19 provides the deceleration of an object at instantaneous velocity v. This result agrees with that given by Fletcher et al. 1966 ($a = 0.8399\ \log_{10}(\mathrm{m}^{b-1}/\mathrm{s})$ and $b = 1.6169$).

given by Equation 2. The final equation for the dimensionless translation model is

$$\frac{dV}{d\widetilde{t}_u} = QA\left(\frac{U-V}{U}\right)^2 - \frac{Ft_u^+}{c_0^{1-B}}\left(\frac{V}{M^{1/6}}\right)^B. \tag{21}$$

3.3.2 Model Verification

To verify the final translation model given by Equation 21, we compare results of our model simulation with results from a LFMER report (Fletcher et al. 1975). In this report Fletcher et al. performed simulations to predict the translational profile of exposed personnel. For each simulation, the peak, positive duration, and impulse of both the overpressure and dynamic pressure are given. Simulations were run for personnel in different initial orientations, including prone and standing. Appendix A.3 gives the R function used to run model simulations to perform the verifications.

To verify the model given by Equation 21, the dynamic pressure wave and time-course of the wind velocity must be specified. Assumptions are required to obtain these inputs because the overpressure and dynamic pressure waveforms were not made explicit in the 1975 report. Thus, these waveforms must be estimated here using the peak, duration, and impulse.

The waveforms for the dimensionless overpressure and dynamic pressure are assumed to be of the following form

$$P = P_s(1-\widetilde{t}_p)e^{-n\widetilde{t}_p} \tag{22}$$

$$Q = Q_s(1-\widetilde{t}_u)e^{-r\widetilde{t}_u}. \tag{23}$$

This is in agreement with equations used in other LFMER reports to define pressure waves (Bowen et al. 1968). Using Equation 22 and 23, the dimensional overpressure impulse (I_p) and the dynamic pressure impulse (I_q) for the positive portion of the blast wave are

$$I_p = \frac{p_s t_p^+}{n^2}(e^{-n}+n-1) \tag{24}$$

$$I_q = \frac{q_s t_u^+}{r^2}(e^{-r}+r-1). \tag{25}$$

For a specific scenario, the value of n and r were determined by solving Equation 24 and 25 since the values for p_s, q_s, I_p, I_q, t_p^+, and t_u^+ are given.

To determine the time-course of the wind velocity, we (1) calculate the temperature at the shock wave front using Rankine-Hugoniot relations,

$$\widetilde{T}_s = \frac{7+P_s}{7+6P_s}(1+P_s) \tag{26}$$

(2) calculate the temperature within the shock wave assuming adiabatic conditions (an assumption that is stated in Fletcher et al. 1975),

$$\widetilde{T} = \widetilde{T}_s\left(\frac{P+1}{P_s+1}\right)^{\frac{\gamma-1}{\gamma}} \tag{27}$$

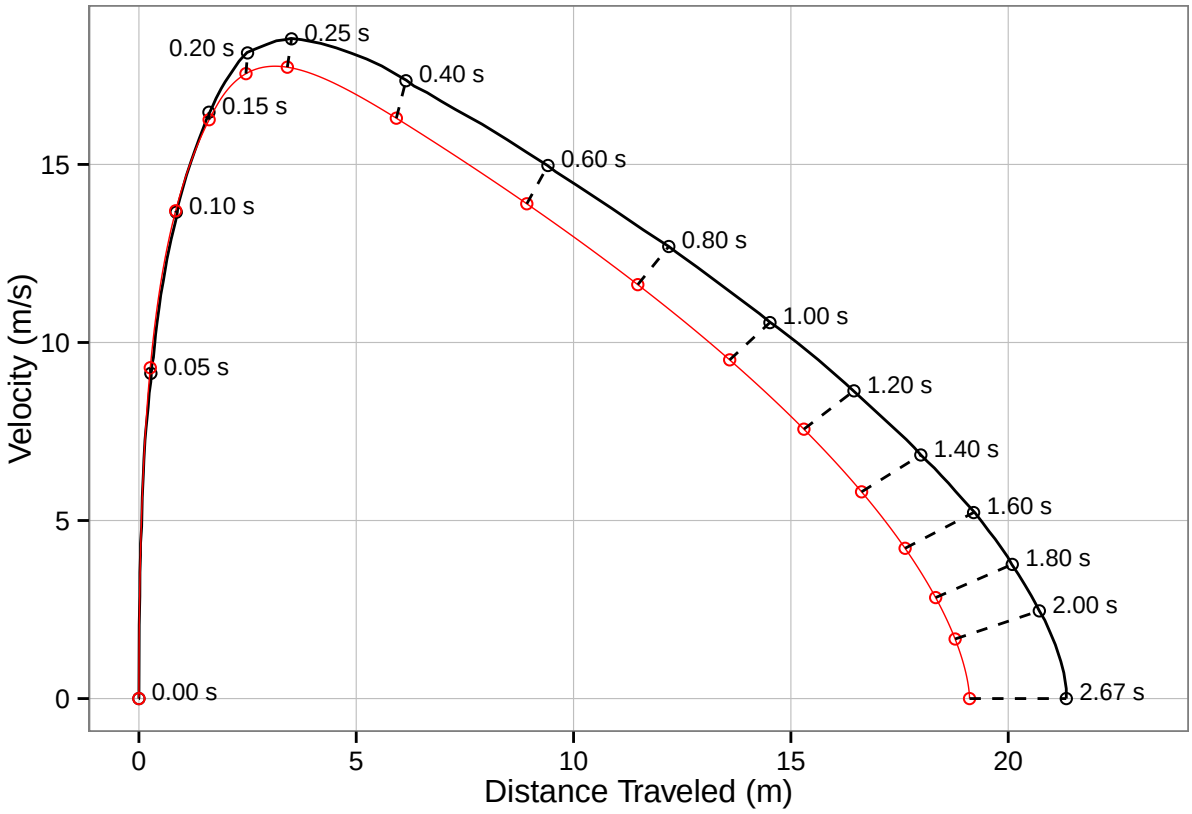

Figure 3.2: Verification of the final translation model. Model simulation (red line/circles) compared with digitized data (black line/circles) obtained from Figure A-1 of Fletcher et al. 1975. The open circles connected by dashed lines represent the same time points post blast wave arrival.

where γ is the adiabatic index for a diatomic gas or 7/5, and (3) calculate the air density.

$$\widetilde{\rho} = \frac{P+1}{\widetilde{T}} \tag{28}$$

Finally, the dimensionless wind velocity can be calculated using $q = \frac{1}{2}\rho u^2$ and the appropriate substitutions (see Section 3.1, Nomenclature):

$$U = \sqrt{\frac{2QRT_0}{c_0^2\widetilde{\rho}}} \tag{29}$$

Equations 22-29 were used to solve Equation 21 numerically. Results comparing our model output with a simulation from Fletcher et al. 1975 are shown in Figure 3.2. This simulation represents the 10^{th} run in the Fletcher 1975 report for a prone personnel in a random orientation. This verification represents a 10 kT surface burst and a ground range of 394 m (1263 ft). The parameters used for this simulation are given in Table 3.2. The

Table 3.2: Parameters used to run verification shown in Figure 3.2.

Parameter	Value
p_s	189 kPa (27.4 psi)
t_p^+	0.355 s
I_p	17.1 kPa s (2.478 psi s)
q_s	96.5 kPa (14 psi)
t_u^+	0.672 s
I_q	7.05 kPa s (1.021 psi s)
R	287.058 J kg^{-1} K^{-1}
T_0	298 K

following equation is used to define α (as specified in Fletcher et al. 1975):

$$\alpha = \begin{cases} 0.0029 \frac{\text{m}^2}{\text{kg}} + \left(\frac{d}{31.65 \text{ kg}^{1/2}}\right)^2 & 0 \leq d \leq 1.8 \text{ m} \\ 0.0061 \frac{\text{m}^2}{\text{kg}} & 1.8 \text{ m} \leq d \end{cases} \tag{30}$$

where d is the distance the object has traveled in meters.

Figure 3.2 shows slight discrepancies between our model output and the translational profile given by Fletcher et al. 1975. Specifically, the peak velocity predicted by our model is slightly lower and the resulting predicted displacement is less. The discrepancies may be caused by the assumed shape of the dynamic and overpressure waveforms or differences between the numerical methods. Given the sources of error, we are satisfied that we have accurately reproduced the translation model with deceleration.

3.4 Validation

We validated the translation model by comparing two sets of displacement data to model predictions. The first set of data relates the dynamic pressure impulse I_q to the displacement of jeeps (Needham 2010), and the second set relates the displacement of pedestrians who have been struck by automobiles to the speed of the automobile during impact (Otte 2001). Appendix A.3 gives the R function used to run model simulations to perform the validations.

3.4.1 Displacement

The dynamic pressure impulse is the only blast wave parameter available for the jeep displacement data (Needham 2010). Therefore, we ran the model with different blast wave parameters subject to the constraint that the dynamic pressure impulse had to equal a specified value. t_u^+ and t_p^+ were varied from 0.1 to 1 s, r and n were varied from 0.1 to 5. Using these values and Equation 4, 22 and 23, we determined P_s and Q_s. We approximated the value of α for a jeep side on as 0.005 m^2/kg ($C_d = 1$, $s = 5$ m^2, $m = 1000$ kg). This process was repeated for dynamic pressure impulses ranging from 0.5 to 100 kPa s. Based on these simulations, we determined the minimum and maximum displacement as a function of the dynamic pressure impulse.

Figure 3.3 compares the predicted displacement ranges to the data on jeep displacement. From this comparison, it is evident that the model is able to accurately predict jeep displace-

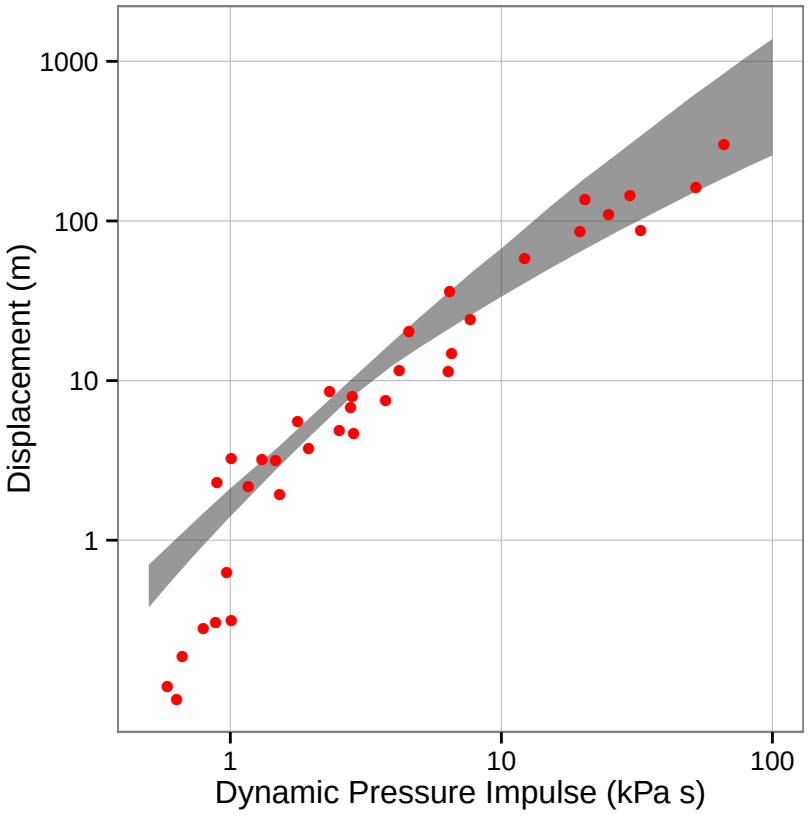

Figure 3.3: Model prediction (shaded region) of jeep displacement range as a function of dynamic pressure impulse. Data (red dots) from Needham 2010.

ment, despite the many assumptions involved in the calculations. However, at lower impulse values (< 1 kPa s), the model overestimates the displacement. This is likely because there is a threshold force required for displacement to occur and the model currently does not take this into account.

3.4.2 Deceleration

For a qualitative validation of the deceleration portion of the model, we compare model predictions to data on pedestrian displacement following car accidents. For forensics purposes, data has been collected on the distance a pedestrian hit by an automobile is thrown as a function of the velocity of the car at impact (Otte 2001). We assume the horizontal velocity of the person immediately after impact is equal to that of the car and compare this data to model predictions (Figure 3.4). In this comparison, the model slightly underestimates the displacement. Because energy is absorbed upon impact, assuming the initial velocity of the pedestrian is equal to that of the car may not be accurate. Furthermore, the model may be overestimating deceleration. The decelerative function was derived by scaling animal data to humans which may result in inaccuracies due to different tumbling dynamics. Also, in the data used for validation, there are uncertainties in the car velocity, pedestrian weight

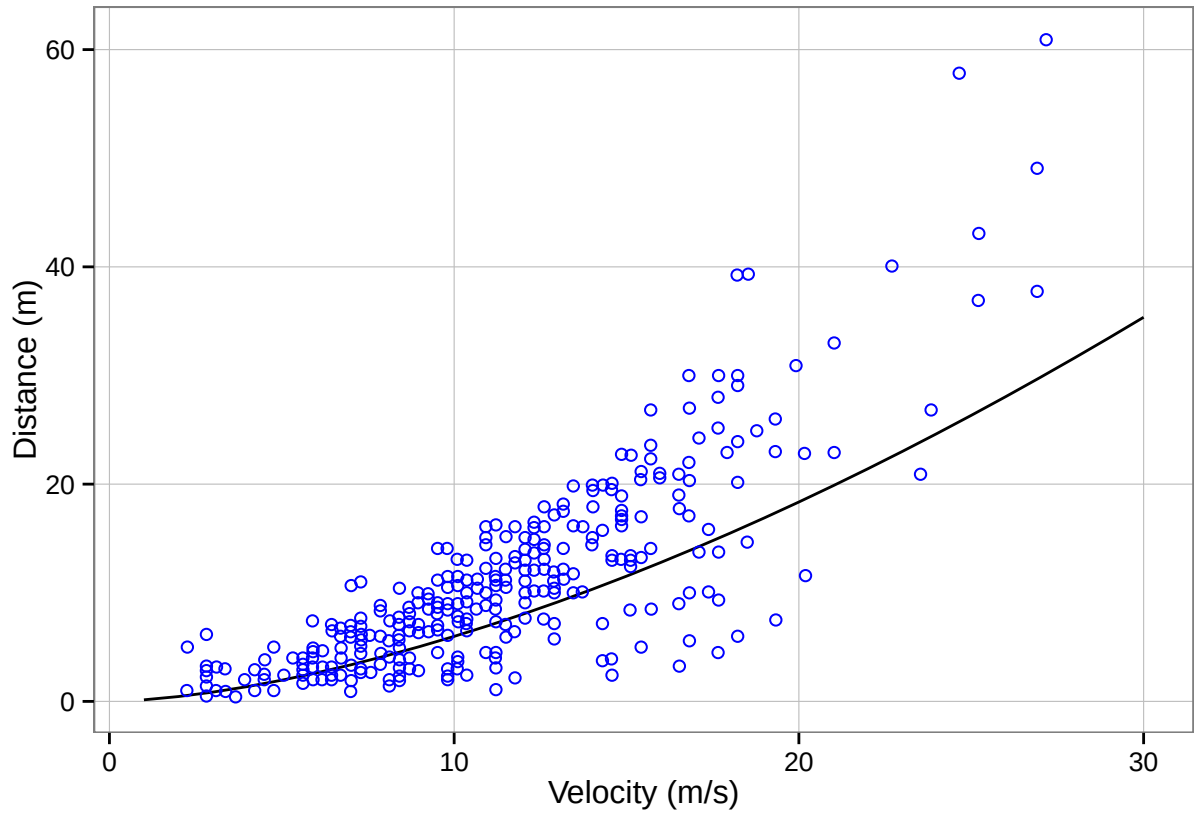

Figure 3.4: Model prediction of pedestrian displacement (black line) compared with car accident data (blue circles; Otte 2001).

(assumed to be 75 kg) and dynamics of the impact (e.g., the height reached by an individual and the time spent in contact with the automobile). Future work will involve looking more critically at accident data, dummy tests, and recent derivations on the relationship between pedestrian velocity and distance thrown to improve upon the translation model or obtain better data for validation (Hague 2001).

4 Injury Probit Models

In this section, we present probit models which relate an object's velocity to the probability of injury due to blast. Existing injury criteria models from the nuclear effects community are reviewed which include models from the 2013 PRCC Report, EM-1 Ch. 14, and a presentation by Dr. John Mercier at the DTRA HRP meetings in the early 2000s (Department of the Army 2013; Drake et al. 1993; Reeves 2015; Mercier 2001). In some cases where ambiguities exist, new probit models are generated.

For each injury type, there are multiple injury levels ranging from moderate to fatal. In Section 4.1, we describe the different injury levels and contemporary methods for ranking injury severity. In Section 4.2, the generic probit model equations are provided as well as methods for calculating uncertainties.

In Section 4.3 and 4.4, we review the existing probit curves relating the probability of tertiary injury to the maximum velocity obtained by the human body. Tertiary injury criteria models exist for decelerative tumbling and perpendicular impact. Existing probits assume decelerative tumbling occurs along a flat, horizontal surface and impact occurs against a perpendicular, non-deformable surface. Other mechanisms of tertiary injury, such as impact against a deformable surface or tumbling down a slope, have not been thoroughly investigated previously. Based on the review of these probits, we decided to generate new probit models for injury due to decelerative tumbling and perpendicular impact.

Section 4.5 and 4.6 discuss secondary injuries caused by penetrating injury and blunt trauma, respectively. The 2013 PRCC report provides injury criteria models for glass and stone penetration. EM-1 Ch. 14 is in general agreement with the PRCC report. We reviewed the source data used by the PRCC report for probit generation. However, we were unable to re-derive the presented penetration probits. Therefore, using the same source data, we developed revised penetration probit models. For blunt trauma, the PRCC report and EM-1 Ch. 14 present the same injury criteria model; however, we were unable to obtain the source documentation for this probit.

4.1 Injury Severity Levels

The probit models discussed represent injury severity levels ranging from moderate to fatal, as described in Table 4.1. Traditionally, separate terminology is used for injury severity levels in military personnel and civilians. For example, injuries resulting in death are termed immediate permanent ineffectiveness (IPI) for military personnel and fatal injury (FI) for civilians (Department of the Army 2013; Jackson et al. 2013). For blast, the main difference

Table 4.1: Injury level definitions.

Injury Level	Description
Fatal Injury (FI)	Injury resulting in death
Serious Injury (SI)	Fractured bones or ruptured internal organs
Moderate Injury (MI)	Multiple lacerations/contusions due to small missiles
Combat Ineffectiveness (CI)	Performance decrement greater than 75%

Definitions obtained from Department of the Army 2013; Jackson et al. 2013.

in terminologies is that military personnel are assumed to be in a prone position while civilians are assumed to be standing upon arrival of the blast wave. Thus, the velocity obtained by a military personnel is less than in a civilian following the same blast wave; however, the velocities that ultimately result in IPI and FI are the same. The injury levels listed in Table 4.1 are those relevant to the probit models under consideration in our work: fatal injury (FI), serious injury (SI), moderate injury (MI), and combat ineffectiveness (CI). According to the PRCC report, 1%, 2.5% and 5% CI correspond to negligible, moderate, and emergency levels of risk (Department of the Army 2013).

In contemporary data, injury levels are often presented using the Injury Severity Score (ISS). The ISS is a scoring system used to assess trauma severity on a whole body level (Baker et al. 1974). The ISS is based upon the Abbreviated Injury Scale (AIS). The AIS classifies an injury based on its location in the body and severity. There are nine possible locations, and the injury severity is categorized using a number ranging from 1 to 6, where a 3 corresponds to a serious injury. The ISS is equal to the squared sum of the highest AIS scores from the three most injured regions of the body. We classify subjects with an ISS score of 9 or greater as having SI. Thus, in some cases, SI data includes subjects with fatal injuries.

4.2 Probit Model Equation

Probit curves relating an input (e.g., velocity and energy) to injury are defined by the PRCC report, EM-1 Ch. 14 and the HRP panel using the following relation (Drake et al. 1993; Reeves 2015; Department of the Army 2013; Mercier 2001):

$$\Phi^{-1}(p_I) = \beta \log_{10}(\frac{x}{X_{50}}) \tag{31}$$

where p_I is the probability of an injury type ranging from 0 to 1, x is the input, β is a dimensionless parameter representing the slope of the probit model, X_{50} is the input at which there is a 50% chance of injury, and Φ is the cumulative normal distribution defined as

$$\Phi(z) = \frac{1}{\sqrt{2\pi}} \int_{-\infty}^{z} e^{-\frac{t^2}{2}} dt. \tag{32}$$

In the generation of new injury criteria models, we will continue to use this same probit function.

The data used to generate probit models for estimating probability of injury can be represented with a binomial distribution where there are n samples and the probability of injury is p_I. The following formula defines the uncertainty associated with the predicted value of p_I:

$$\sigma^2 = \frac{p_I(1-p_I)}{n} \tag{33}$$

where σ is the standard deviation. In this report, we use this formula to give the error on probability estimates.

For tertiary injury, due to the range of probit models that will be discussed, the following notation will be used. $V_{i,j,k}$ will refer to the velocity at which there is an i percent probability of injury j due to k. Where $i = 0$ to 100, j equals the injury levels (i.e., FI, CI, SI, and MI), and k is the injury type (DT for decelerative tumbling and PI for perpendicular impact). Similarly, the slopes of probits will be represent as $\beta_{j,k}$.

4.3 Decelerative Tumbling

There are several probit models which calculate the probability of injury due to decelerative tumbling as a function of the maximum velocity obtained. Due to limitations in data, the existing probit models are based on extrapolations from animal experiments. EM-1 Ch. 14 provides probit models for FI and SI, and the 2013 PRCC report provides a probit model for CI. Dr. Mercier presented probit models for FI, SI, and MI at the the HRP meetings. Due to ambiguities and assumptions underlying existing probits, new probits were generated here using motorcycle accident data to represent injury likelihood in urban environments. Table 4.2 provides the probit equations for all the decelerative tumbling probit models.

Table 4.2: Probit models for injury due to decelerative tumbling.

Injury Level	Source	Probit Equation	Data/Assumptions
FI	EM-1 Ch. 14 (Reeves 2015)	$19.55 \log_{10}(v/V_{50})$ V_{50}=45.11 m/s	Assumes 5% probability of FI is equal to 95% probability of SI. Assumes slope is same as EM-1 Ch. 14 FI perpendicular impact probit.
	HRP (Mercier 2001)	$19.52 \log_{10}(v/V_{50})$ V_{50}=44.39 m/s	No information on probit generation methodology or source data given.
	ARA	$2.86 \log_{10}(v/V_{50})$ V_{50}=40.19 m/s	Based on motorcycle accident data (Hurt et al. 1981a)
SI	EM-1 Ch. 14/HRP (Reeves 2015)	$6.42 \log_{10}(v/V_{50})$ V_{50}=20.24 m/s	Based on sheep data (source data reference unknown).
	ARA	$2.40 \log_{10}(v/V_{50})$ V_{50}=9.22 m/s	Based on motorcycle accident data (Hurt et al. 1981a)
MI	HRP (Mercier 2001)	$6.42 \log_{10}(v/V_{50})$ V_{50}=17.51 m/s	No information on probit generation methodology or source data given.
CI	PRCC (Department of the Army 2013)	$5.40 \log_{10}(v/V_{50})$ V_{50}=23.16 m/s	Derived using goat data (Anderson et al. 1961). Assumes slope is the same as PRCC CI perpendicular impact probit.

Table 4.3: Verification of probit model for CI due to decelerative tumbling.

	Reported by PRCC*	Calculated
Velocity → 1% CI (Negligible Risk)	9.1 m/s	8.5 m/s
Velocity → 2.5% CI (Moderate Risk)	10.7 m/s	10.1 m/s
Velocity → 5% CI (Emergency Risk)	11.9 m/s	11.6 m/s

*Obtained from Department of the Army 2013.

4.3.1 PRCC Report

The PRCC report provides a probit curve for CI due to decelerative tumbling (Table 4.2). The $V_{50,CI,DT}$ is given in the PRCC report (23.16 m/s), and the slope $\beta_{CI,DT}$ was derived[3]. To verify the implementation of this probit model, the velocities which result in 1%, 2.5% and 5% CI were calculated using the probit model and compared to the velocity values given in the PRCC report (Table 4.3). These values are within ± 0.6 m/s of each other.

There were two major assumptions in the CI probit model development: (1) injury data was extrapolated directly from animals to humans (i.e., the velocity that led to 33% CI in goats was assumed to be the same as the velocity that led to 33% CI in humans) and (2) because of the limited animal data, the probit slope for CI due to decelerative tumbling was assumed to be equal to the slope of the perpendicular impact CI probit ($\beta_{CI,DT} = \beta_{CI,PI}$).

The source data for the injury criteria model came from a blast wave study (Anderson et al. 1961). In this study, animals were placed in different orientations and locations within a blast tube and subjected to a blast wave. Their subsequent maximum velocity was recorded. The animals were classified as injured if they were paralyzed or died. Upon review of the primary study, it became clear that all the animals classified as injured died within a few hours of blast. This suggests that the data from this study may be more applicable for estimating the likelihood of mortality. The PRCC report used this study to report a 33% CI probability for a velocity of 19.2 m/s (range: 16.5-23.8 m/s). However, we were unable to derive these parameters from the original source data (Anderson et al. 1961).

4.3.2 EM-1 Ch. 14

EM-1 Ch. 14 provides probit curves for SI and FI due to decelerative tumbling. The probit equation for SI is not explicitly stated in EM-1 Ch. 14 but is rather shown in Figure 60 (Reeves 2015). A probit equation given in a LFMER report (Fletcher et al. 1975) was found to match the SI probit curve shown in EM-1 Ch. 14 (see Table 4.2 for equation). EM-1 Ch. 14 and the Fletcher et al. 1975 study both reference the Middle North Series reports as the source for the SI probit model (Richmond et al. 1974a; Richmond et al. 1974b). However,

[3]In the PRCC report, the velocity for 33% and 50% CI due to decelerative tumbling are provided ($V_{33,CI,DT}$ = 19.20 m/s and $V_{50,CI,DT}$ = 23.16 m/s). Using this information and Equation 31, we back-calculate the probit model slope:

$$\beta_{CI,DT} = \frac{\Phi^{-1}(0.33)}{\log_{10}(V_{33,CI,DT}/V_{50,CI,DT})} \tag{34}$$

where $\Phi^{-1}(0.33) = -0.4399132$

upon review of these published references, no decelerative tumbling data were found. Due to a lack of a clear reference to the source data for generation of this probit, we cannot verify the basis on which the probit was developed.

The FI probit curve presented in EM-1 Ch. 14 was derived using assumptions given in Drake et al. 1978 (see page 5-99). These include (1) a 95% probability of SI is equivalent to a 5% probability of FI, and (2) the slopes of the probits for FI due to decelerative tumbling and perpendicular impact are equal ($\beta_{FI,DT} = \beta_{FI,PI} = 19.55$, see Section 4.4.2 for the perpendicular impact probit slope source). Using the SI probit given in Table 4.2, a maximum velocity of 36.6 m/s would result in 95% probability of SI. Thus, for the FI probit, $V_{05,FI,DT} = 36.6$ m/s. In turn, $V_{50,FI,DT} = 45.11$ m/s[4]. However, as stated previously, due to the uncertainty of the SI probit, the derived FI probit is also questionable.

4.3.3 HRP

Three probit models for decelerative tumbling were presented by Dr. Mercier at the HRP meetings in the early 2000s (Mercier 2001). These include models for FI, SI, and MI. The probit parameters for injury due to decelerative tumbling are given in Table 4.2.

The SI probit matches that given in EM-1 Ch. 14, and the FI probit is very similar to the EM-1 Ch. 14 probit. Mercier cited Fletcher et al. 1975 and Drake et al. 1978 as references for the SI and FI probits. The MI probit developed by Mercier has the same slope as the EM-1 Ch. 14 SI probit but a slightly lower velocity leading to 50% injury (17.5 m/s compared with 20.2 m/s). Mercier reports that the MI probit is based on both sheep data and human jumper data; however, no source references are provided. We note that human jumper data would be more applicable to impact injuries.

4.3.4 AMedP-8

The AMedP-8(C) NATO planning guide of 2009 provides information on FI due to the decelerative tumbling caused by blast (NATO 2009). In this reference, 50% FI for a prone personnel in a random orientation is related directly to yield and static overpressure. NATO derived this relationship using a log-linear interpolation and three data points obtained from Drake et al. 1978. Drake et al. calculated these data points using the look-up tables from Fletcher et al. 1975; however, the specific velocity which leads to the 50% FI rate is not provided. Using the Tables A-1 and A-3 from Fletcher et al. 1975, the V_{50} velocity used must be between 33.5 m/s and 43.0 m/s.

The relationship between blast parameters and FI given in AMedP-8 was developed using the same methodologies as EM-1 Ch. 14 and the PRCC report. However, fewer data points were used (i.e., only data points on the overpressure values at 1, 10, 100 kT required to produce 50% FI). AMedP-8 does not provide information on a probit slope.

[4]

$$V_{50,FI,DT} = \frac{V_{05,FI,DT}}{10^{\Phi^{-1}(0.05)/\beta_{FI,DT}}} \tag{35}$$

where $\Phi^{-1}(0.05) = -1.644854$.

Table 4.4: Motorcyclist post-crash motion.

Post-Crash Motion	Percent of Motorcyclists Examined
Stopped near point of impact	9.1%
Vaulted from motorcycle	26.7%
Fell from motorcycle	25.9%
Tumbled or rolled	12.8%
Slid to a stop	11.4%
Trapped under motorcycle	8.8%
Trapped under other vehicle	2.3%
Struck and dragged by other vehicle	1.2%

Data obtained from Table 8.3.2 of Hurt et al. 1981a.

4.3.5 Probit Generation

Because the decelerative tumbling probits provided in the PRCC report and EM-1 Ch. 14 were based on very limited animal data with large inherent uncertainties, we initiated a search for better data sources. Motorcycle accidents, although highly uncontrolled, provide a representation of what might be observed in an urban environment following exposure to a blast wave. However, we would not expect this data to represent injuries in open field environments. Thus, we propose to use the probits generated from motorcycle accident data to predict injury only in urban environments.

We examined a study on motorcycle accidents done for the U.S. Department of Transportation in 1981 (Hurt et al. 1981a). This study contains data on 900 motorcycle accidents and includes details on injury severity, collision speeds, helmet use, and post-crash motion. Data from motorcycle accidents represent several different types of injury due to contact with the motorcycle, other vehicles, or stationary objects. For 884 out of the 900 motorcyclists examined, the motorcyclist post-crash motion is given (Table 4.4). 76.8% of the data came from motorcyclists who vaulted from motorcycle, fell from motorcycle, tumbled/rolled, or slid to a stop. 40% of the motorcyclists in the study were wearing helmets. Table 4.5 contains injury versus crash speed data derived from the motorcycle accident study. Injury

Table 4.5: Proportion of motorcyclists with SI and FI as a function of crash velocity.

Midpoint (range) of crash speeds (m/s)	Total Motorcyclists	Number (%) with SI*	Number (%) with FI**
2.34 (0-4.47)	83	24 (28.9%)	1 (1.2%)
6.71 (4.92-8.94)	349	123 (35.2%)	7 (2.0%)
11.18 (9.39-13.41)	270	166 (61.5%)	9 (3.3%)
15.65 (13.86-17.88)	129	92 (71.3%)	18 (14.0%)
20.12 (18.33-22.35)	32	26 (81.3%)	6 (18.8%)
24.59 (22.80-26.82)	24	17 (70.8%)	8 (33.3%)
29.06 (27.27-31.29)	9	7 (77.8%)	4 (44.4%)
33.53 (31.74-35.76)	2	2 (100%)	0 (0%)

*Derived from Table 8.8.6 from Hurt et al. 1981a where SI is equivalent to an SS$\geq$6.
**Derived from Table 8.8.3 and Table 8.8.5 from Hurt et al. 1981b.

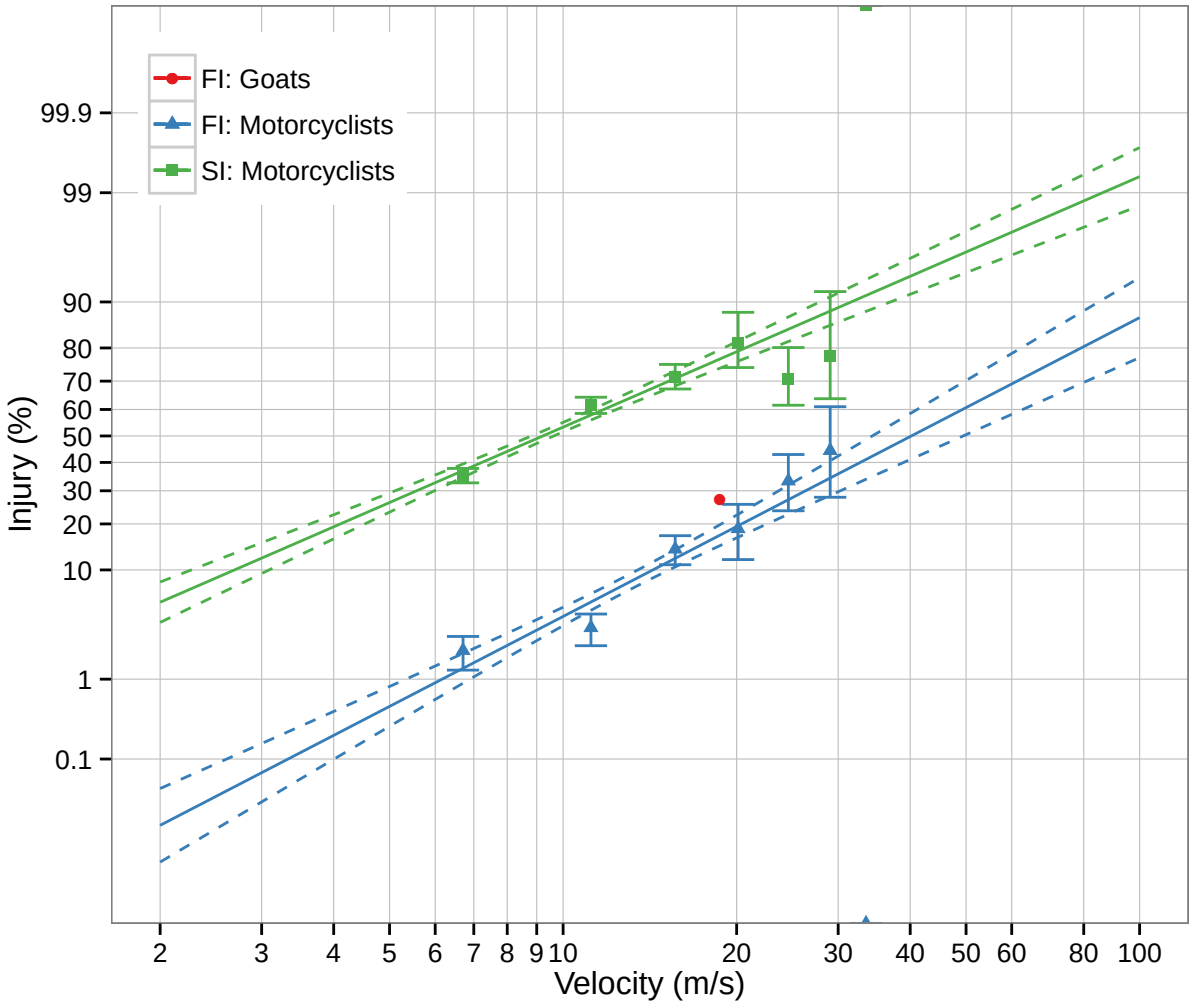

Figure 4.1: Comparison of motorcycle probits for FI and SI with data (Hurt et al. 1981a). Goat data derived from Anderson et al. 1961.

levels were quantified in the study using a "Severities Sum" (SS) score, where an SS score of 6-12 corresponds to an AIS of 3 (Hurt et al. 1981a). Thus, we classify subjects with SS scores of 6 or greater as seriously injured.

Probits for FI and SI as a function of velocity were generated. The probit models were parameterized using the data given in Table 4.5. However, we excluded the lowest velocity group ($\leq$4.47 m/s) because 20% of these accidents occurred at a crash velocity of 0 m/s. This indicates that other injury types besides decelerative tumbling significantly contributed to the injuries observed in this group (e.g., crushed by motorcycle and struck by another vehicle). While injuries unrelated to decelerative tumbling may be included in other velocity groups, we do not anticipate that they impact the injury curve as dramatically as expected in the slower velocity group. Because individual crash speeds were not given, we used the midpoint of the velocity range for each group as the crash velocity. Figure 4.1 shows the probits overlaid on the accident data along with the 95% confidence interval. The data

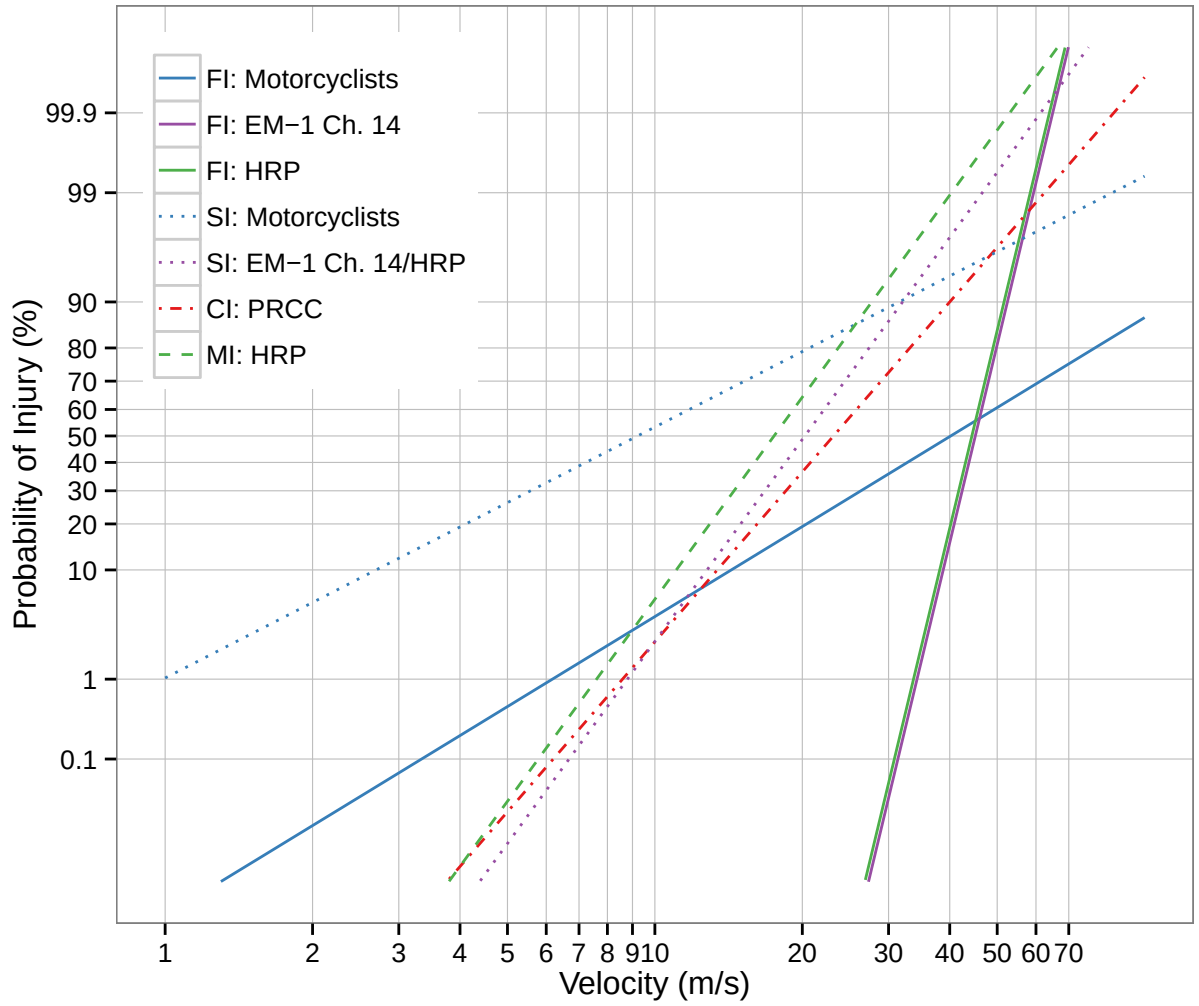

Figure 4.2: Decelerative tumbling probits.

point derived from the decelerative tumbling study in goats is also shown (Anderson et al. 1961). In this study, 15 goats obtained a velocity between 16.6 and 20.6 m/s with an average velocity of 18.7 m/s. Of these goats, 4 died, leading to mortality rate of 27%[5]. The FI probit generated from motorcyclist data is consistent with the data point from the goat tumbling study.

4.3.6 Analysis

Figure 4.2 shows a comparison of all the decelerative tumbling injury criteria models. The V_{50} for FI obtained using motorcyclist data is between the V_{50} for FI from EM-1 Ch. 14 and the V_{50} for CI from the PRCC report (see Table 4.2). The PRCC CI probit model is

[5]In the Anderson study, one of the goats obtained a velocity of 23.7 m/s. However, because the 4 goats who died had a mean velocity of 18.0 m/s, we were able to determine that the goat at 23.7 m/s did not die and exclude it, thereby limiting the velocity range.

comparable to the FI probit models since all the goats in the source data classified as injured died (Anderson et al. 1961). One report uses the FI probits from EM-1 Ch. 14 and the PRCC report to estimate a V_{50} of 34.7 m/s (Drake et al. 1978), which falls into the 95% confidence interval predicted by the probit derived using motorcycle accident data (see Figure 4.1). The V_{50} for SI, obtained using motorcyclist data, is much less than that predicted by EM-1 Ch. 14 (see Table 4.2). The SI probit from EM-1 Ch. 14 is based on sheep data and Drake et al. 1978 notes that sheep are a round animal which tend to roll upon impact with the surface. This suggests sheep can withstand a higher velocity than humans prior to injury. Thus, a lower V_{50} than that predicted with sheep data is not unrealistic.

The probit slopes obtained with the motorcycle accident data are significantly less than the slopes of the EM-1 Ch. 14, PRCC, and HRP probit models (see Figure 4.2). When two probit models have different slopes, this inherently implies that there is a threshold velocity at which the probits cross. For example, comparing the motorcycle probits with the EM-1 Ch. 14 probits, this threshold velocity is equal to 32.37 m/s for SI and 46.01 m/s for FI. Below this threshold, the motorcycle probits predict a higher probability of injury than the EM-1 Ch. 14 probits. Above this threshold, the motorcycle probits predict a lower probability of injury than the EM-1 Ch. 14 probits. The EM-1 Ch. 14, PRCC, and HRP probit models are meant to predict injury due to decelerative tumbling in open field environments. Meanwhile, the motorcycle accident data represents a more complex environment due to interactions of the body with the motorcycle and other objects. Thus, the motorcyclist data are more applicable for urban scenarios. Due to the complex nature of urban environments, a higher probability of injury at lower velocities would be expected. However, at higher velocities, one would not expect the likelihood of injury to be less than that observed in the open field. The source of this discrepancy at higher velocities could arise from two sources: errors in the slopes of the open field probits or the limitations of using a probit type model in representing a more complex injury mechanism. Regarding potential errors in the slopes of the open field probits, the PRCC CI and the EM-1 Ch. 14 FI probit slopes were assumed to equal that of the perpendicular impact probits. However, during decelerative tumbling, multiple impacts occur, and the slope of the probit represents this physical process (Drake et al. 1978). Assuming perpendicular and decelerative probit slopes are equivalent may not be an accurate assumption.

To predict injury due to decelerative tumbling in open field environments, we recommend implementing the probits from EM-1 Ch. 14 into HENRE 2.0. The EM-1 Ch. 14 probits were chosen instead of the probits presented by Dr. Mercier because they have been published and are, thus, better documented. All of the preexisting decelerative tumbling probits reviewed here have similar issues regarding the availability of data, details on methodologies, and/or quality of data used in their development. The animals used to generate the probit models (i.e., goats and sheep) are quadrupedic, meaning the mechanics of how they tumble is different than that in bipeds (i.e., humans). In some experiments, the animals used were anesthetized which likely affects the tumbling dynamics. Finally, the animal data used is very limited and does not involve a wide range of velocities which leads to large uncertainties in the probit slopes.

To predict injury in urban environments, we recommend merging the motorcycle accident probits with the EM-1 Ch. 14 probits. Motorcycle accidents, although containing other injury types and in some cases involving head protection and medical treatment, are more

representative of the chaotic state that would occur following blast in an urban environment. However, motorcyclist data was only available up to about 30 m/s. At higher velocities, the predicted injury from EM-1 Ch. 14 is greater than that predicted using motorcycle accident data. Although the motorcycle accident probits show a good match to the available data (see Figure 4.1), it is possible that at higher velocities the probit models do not adequately predict the injury response. Specifically, at a threshold velocity, the probability of injury likely begins increasing more rapidly; however, a simple probit model is not able to capture this effect. Thus, we propose using the motorcycle accident probit at low velocities and the EM-1 Ch. 14 probit at high velocities to predict injury in urban environments. The transition between the two occurs where the probits cross. This threshold velocity is $v = 46.01$ m/s for FI and $v = 32.37$ m/s for SI. Due to limited data, we believe the EM-1 Ch. 14 probit provides the best representation of this transition.

The finalized models for FI and SI in both urban and open field environments will be implemented in HENRE 2.0. In order to avoid any discrepancies, we do not recommend the inclusion of probits for other injury types at this point (i.e., MI and CI).

4.4 Perpendicular Impact

In this section, we analyze existing probits relating impact velocity to injury caused by perpendicular impact with a nonyielding surface. Again probits from EM-1 Ch. 14, the 2013 PRCC report, and PDCALC v8.1 were analyzed and are discussed below. Furthermore, due to ambiguities with the data, we again generated new probit models using more contemporary data. Table 4.6 provides a complete list of probit models for perpendicular impact.

4.4.1 PRCC Report

The PRCC report used data from a 1965 study on human jumpers to determine the likelihood of FI as a function of impact velocity (Lewis et al. 1965). This study provides survival data for 53 subjects who jumped from heights ranging from 3 to 16 stories. The probit indicates a $V_{50,FI,PI}$ of 18.08 m/s with a $\beta_{FI,PI}$ of 5.40. The PRCC report assumes (1) translational velocities associated with 1% mortality correspond to 50% CI and (2) the CI probit model slope is equal to that of the FI probit model ($\beta_{CI,PI} = \beta_{FI,PI}$). Using this information the probit model for CI due to perpendicular impact is fully specified (see Table 4.6).

To verify the probit model, the velocities which result in 1%, 2.5%, and 5% CI due to impact with a perpendicular, nonyielding surface were calculated using the probit model and compared to the velocity values given in the PRCC report (Table 4.7). These values are all

Table 4.6: Probit models for injury due to perpendicular impact.

Injury Level	Source	Probit Equation	Data/Assumptions
FI	EM-1 Ch. 14 (Drake et al. 1993)	$19.55 \log_{10}(v/V_{50})$ V_{50}= 10.70 m/s	Based on sheep data (Richmond et al. 1974a). Source data could not be found.
	PRCC (Department of the Army 2013)	$5.40 \log_{10}(v/V_{50})$ V_{50}= 18.08 m/s	Based on human data (Lewis et al. 1965).
	HRP (Mercier 2001)	$13.29 \log_{10}(v/V_{50})$ V_{50}= 10.82 m/s	No information on probit generation methodology or source data given.
	ARA	$7.19 \log_{10}(v/V_{50})$ V_{50}= 15.35 m/s	Based on human data (Lapostolle et al. 2005).
SI	EM-1 Ch. 14 (Drake et al. 1993)	$6.21 \log_{10}(v/V_{50})$ V_{50}= 4.69 m/s	Based on sheep data (Richmond et al. 1974a).
	HRP (Mercier 2001)	$6.21 \log_{10}(v/V_{50})$ V_{50}= 5.49 m/s	No information on probit generation methodology or source data given.
	ARA	$4.84 \log_{10}(v/V_{50})$ V_{50}= 8.61 m/s	Based on human data (Beale et al. 2000; Dickinson et al. 2012).
MI	HRP (Mercier 2001)	$5.93 \log_{10}(v/V_{50})$ V_{50}= 4.88 m/s	No information on probit generation methodology or source data given.
CI	PRCC (Department of the Army 2013)	$5.40 \log_{10}(v/V_{50})$ V_{50}= 6.71 m/s	Assumes 1% mortality corresponds to 50% CI and the probit slope is the same as the PRCC FI impact probit slope.

Table 4.7: Verification of probit model for CI due to perpendicular impact.

	Reported by PRCC*	Calculated
Velocity → 1% CI (Negligible Risk)	2.6 m/s	2.5 m/s
Velocity → 2.5% CI (Moderate Risk)	3.0 m/s	2.9 m/s
Velocity → 5% CI (Emergency Risk)	3.4 m/s	3.4 m/s

*Obtained from Department of the Army 2013.

within ±0.1 m/s.

4.4.2 EM-1 Ch. 14

EM-1 Ch. 14 presents probits for FI and SI due to perpendicular impact, citing Richmond et al. 1974b as the source (Drake et al. 1993). Although this source did not include injury criteria, data from a companion document (Richmond et al. 1974a) provided probits for FI and SI (see Table 4.6). The probits were calculated using studies in which sheep were dropped from heights of 0.30 to 7.6 m on to a concrete surface. Animals were dropped in five different orientations: head down, tail down, prone, supine, and right side down. SI was defined as the occurrence of fractures, severe organ rupture (liver, heart or major vessel) and death. An impact velocity of 4.9 m/s led to a 50% incidence of SI, and an impact velocity of 8.11 m/s led to a 1% incidence of FI.

4.4.3 HRP

At the HRP meetings, Dr. Mercier presented a probit model for FI due to perpendicular impact (Mercier 2001). Similar to the 2013 PRCC report, this probit was derived with human jumper data from Lewis et al. 1965. However, Dr. Mercier made manual adjustments to the derived probit by reducing the V_{50} by 4.57 m/s (15 ft/s) and increasing the slope by 48%. The V_{50} was reduced to account for a random orientation at impact rather than a feet first orientation, with the underlying assumption that the Lewis et al. study represents predominately feet first falls. No justification for the choice of 4.57 m/s was given. The increased slope was based on sheep data, but, again, the source of the sheep data and the reason for choosing the 48% quantity was not provided. The finalized probit is given in Table 4.6.

We can back-calculate to examine the probit obtained by Dr. Mercier using only the human jumper data (i.e., add 4.57 m/s to the V_{50} and divide the slope by 1.48):

$$\Phi^{-1}(p) = 8.979 \log_{10}(\frac{v}{V_{50}}) \tag{36}$$

where $V_{50} = 15.39$ m/s. Since this probit and the 2013 PRCC probit for FI were derived with the same data, we would expect them to match; however, this is not the case. This discrepancy exists because Dr. Mercier only used data points that represented greater than 10 subjects while the PRCC report likely used all data points. Table 4.8 gives the velocity and mortality data for jumpers where the mortality for the height fallen was greater than 0% and less than 100%. Mercier used only data from jumpers who fell from 3, 4, and 6 stories

Table 4.8: Velocity and mortality data for human falls from heights.

Height in Stories	Velocity (m/s)	Mortality %	Number
3	13.39	33	15
4	16.40	64	11
5	18.93	22	7
6	21.17	91	11
7	23.13	50	2

Data obtained from Lewis et al. 1965.

(Mercier 2001). The inclusion of data from jumpers from 5 and 7 stories would result in a reduced probit slope as seen in the PRCC probit for FI due to impact.

At the HRP meetings, Dr. Mercier also presented probits relating impact velocity to SI and MI. Dr. Mercier's presentation states these probits are based on sheep and human jumper data, but the derivation is not given. The SI probit for impact has the same slope as that given by EM-1 Ch. 14; however, the V_{50} is greater.

4.4.4 Probit Generation

Because the probits reviewed were based on sheep data or obtained from studies on human falls with limited details, we sought to generate probits for SI and FI due to perpendicular impact using contemporary free fall studies. Only data from studies that included adults, out-of-hospital mortality, and both fatal and non-fatal accidents were considered in the generation of revised impact probit models. Many studies provide mortality or injury as a function of height. To determine the corresponding impact velocity, we use the formula: $v = \sqrt{2hg}$ where h is the height and g is the acceleration due to gravity (9.8 m/s^2).

A study on free fall victims in France was used to generate a probit model for FI due to impact (Lapostolle et al. 2005). This study included patients who fell from a height of greater than 3 m and excluded patients less than 12 years of age. A total of 287 patients were included in the analysis. This study was chosen to generate the probit because it contained information on many aspects of the fall, including the circumstances of the fall (i.e., suicide attempt, accident, or escape), whether the impact surface was hard or soft, if there was preliminary impact before final impact, and the part of the body that touched the ground first (i.e., head, lower extremities, posterior, anterior, or lateral). For our purposes, the ideal dataset would involve a hard surface, there would be no preliminary impact before final impact, and an even distribution of parts of the body would touch the ground first. In the study, 72% of the impacts were against a hard surface, and in 83% of the cases there was no preliminary impact before the final impact. Of the patients included in the study, 25% were head first, 24% were feet first, and 37% had a side impact (posterior, anterior, or lateral). In the remaining subjects, the orientation was unknown. Other studies did not provide as detailed information on the circumstances of the falls (Lewis et al. 1965; Beale et al. 2000) and, therefore, were not used in the FI probit generation.

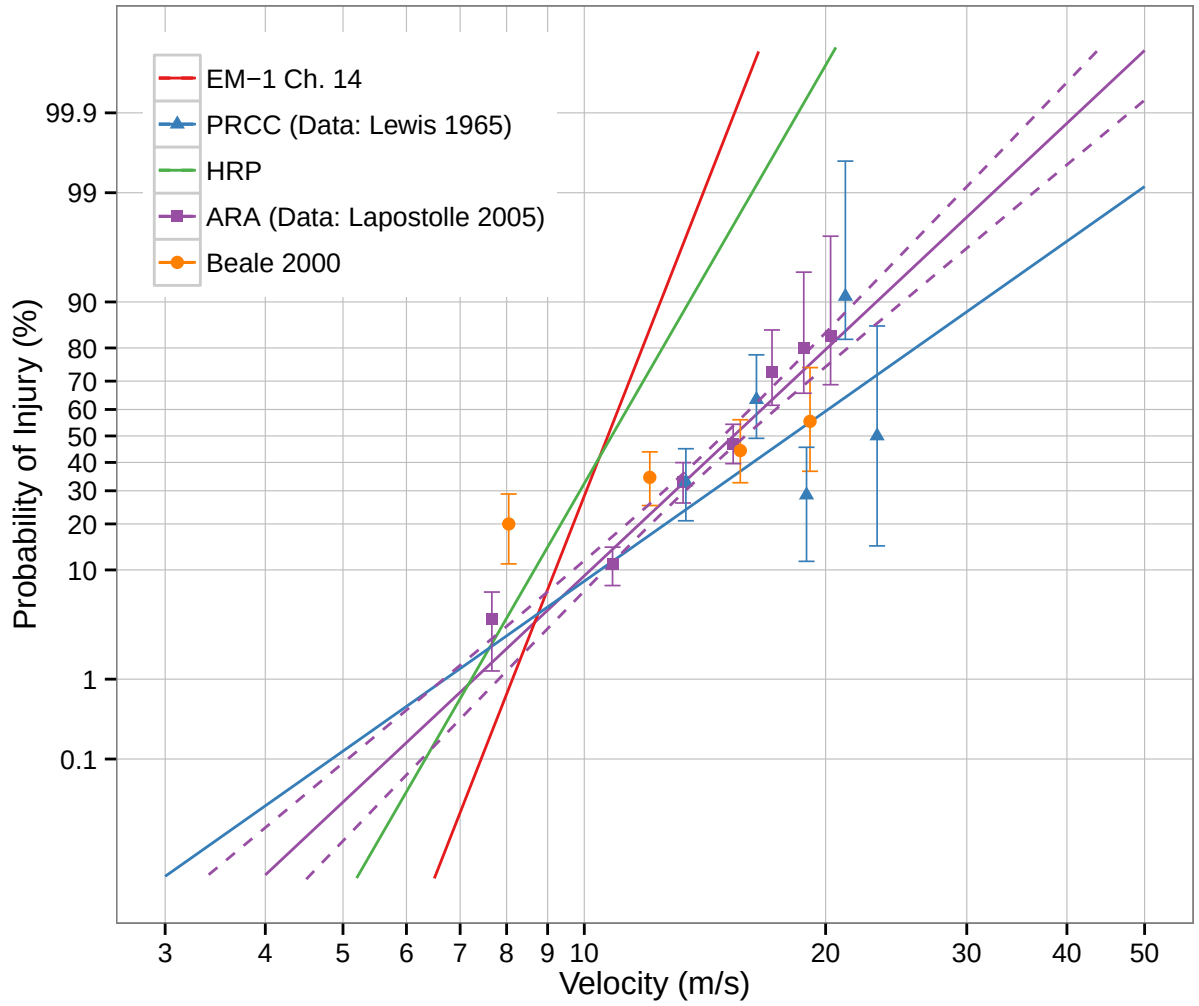

Figure 4.3: Probit models for FI due to perpendicular impact compared with data.

Figure 4.3 shows the FI probit and the 95% confidence intervals along with the data from the Lapostolle et al. study used to generate the probit. For comparison, data from other free fall studies are shown (Lewis et al. 1965; Beale et al. 2000) along with existing probits. The probit model shows a reasonable fit to the data that was used in the generation of the PRCC probit model (Lewis et al. 1965). The data from Beale et al. suggests the probit model should have a smaller slope.

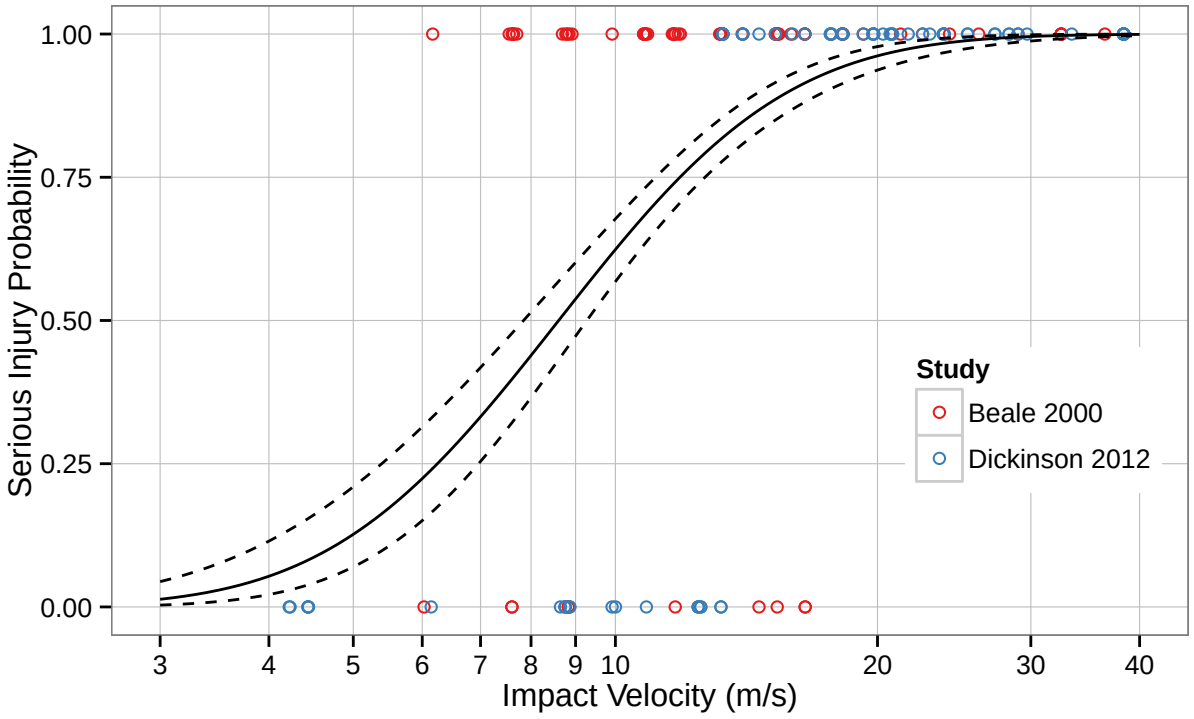

Figure 4.4: Generated SI probit model for perpendicular impact compared with data.

For generating a probit for SI due to impact, we again examined free fall studies. Although the study used for the FI probit generation contained more detailed information, it did not include injury severity data as a function of height. Two other studies, comparable in quality, were found which supplied individual ISS data for both fatal and non-fatal injuries, including patients who died out-of-hospital (Beale et al. 2000; Dickinson et al. 2012). Figure 4.4 shows the probit model obtained through analyzing the individual data.

4.4.5 Analysis

Figure 4.5 compares all the FI perpendicular impact injury criteria models, and Figure 4.6 compares all the SI, MI, and CI perpendicular impact injury criteria models. The probits presented by EM-1 Ch. 14 are based on sheep data, while the PRCC probit and the probits generated here are based on human data. Due to the large physical differences between human and sheep, it is likely that the same impact velocity would result in different injuries. Thus, it is best to use human data, if available, for generating the probit. However, one criticism of the human data used is that the orientation of jumpers would likely result in a feet first landing (Drake et al. 1978), and following a nuclear blast scenario the orientation of body during impact would be more random. The study used by the PRCC report does not provide information on the orientation of the subjects upon impact (Lewis et al. 1965). If impact was predominately feet first, the reported V_{50} value for FI of 18.08 m/s is likely too high because the legs would allow the body to decelerate before major organs or the head

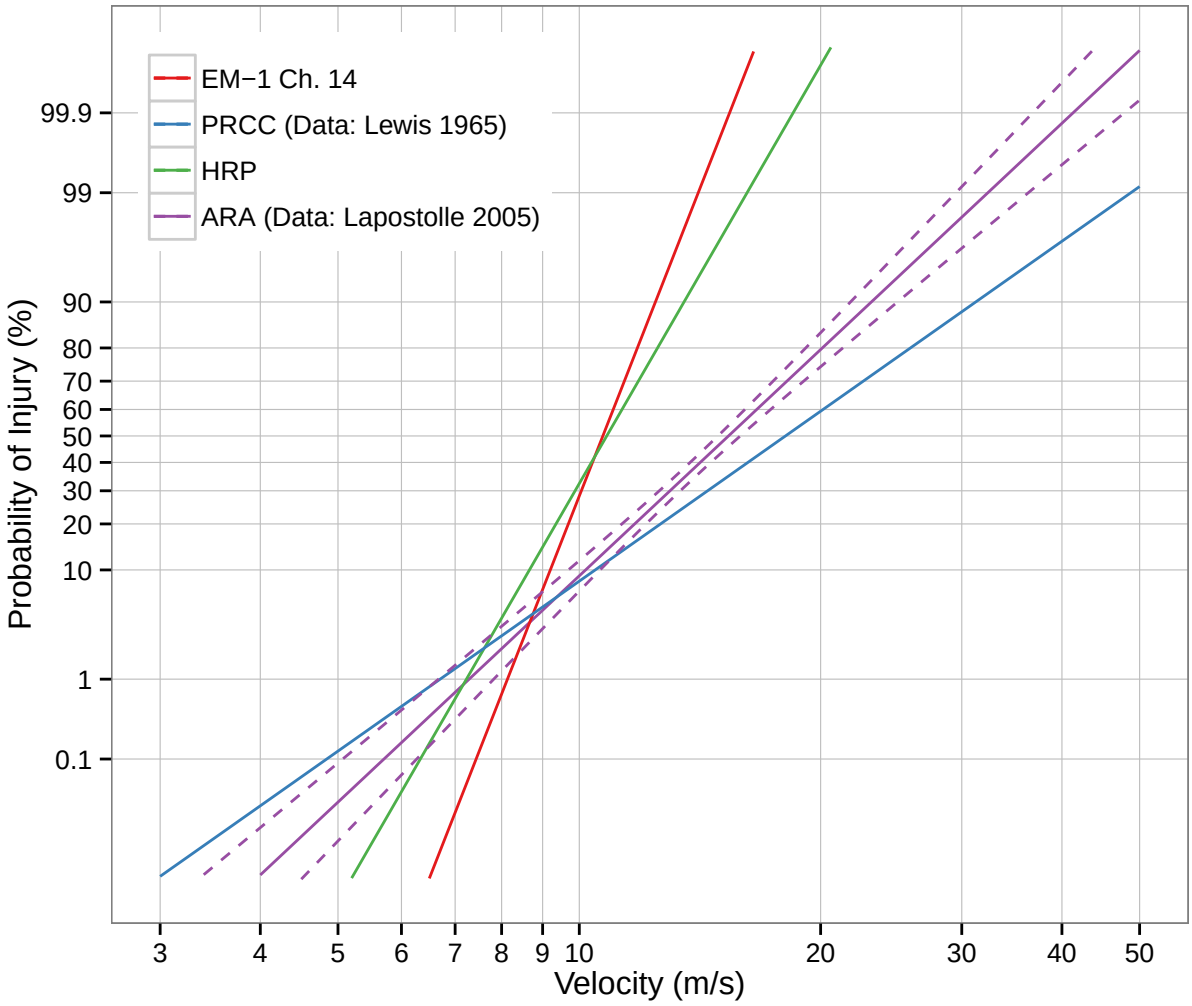

Figure 4.5: Probit models for FI due to perpendicular impact.

impacted the ground.

Rather than revert to sheep data, we decided to search the literature for more recent studies on human falls to generate revised probit models. The probit generated here for FI due to impact falls between the probits given by EM-1 Ch. 14 and the PRCC report (see Figure 4.5). The V_{50} is greater than that predicted by EM-1 Ch. 14 and less than that predicted by the PRCC report (Table 4.6). The slope β is greater than that from the PRCC report and less than that from EM-1 Ch. 14.

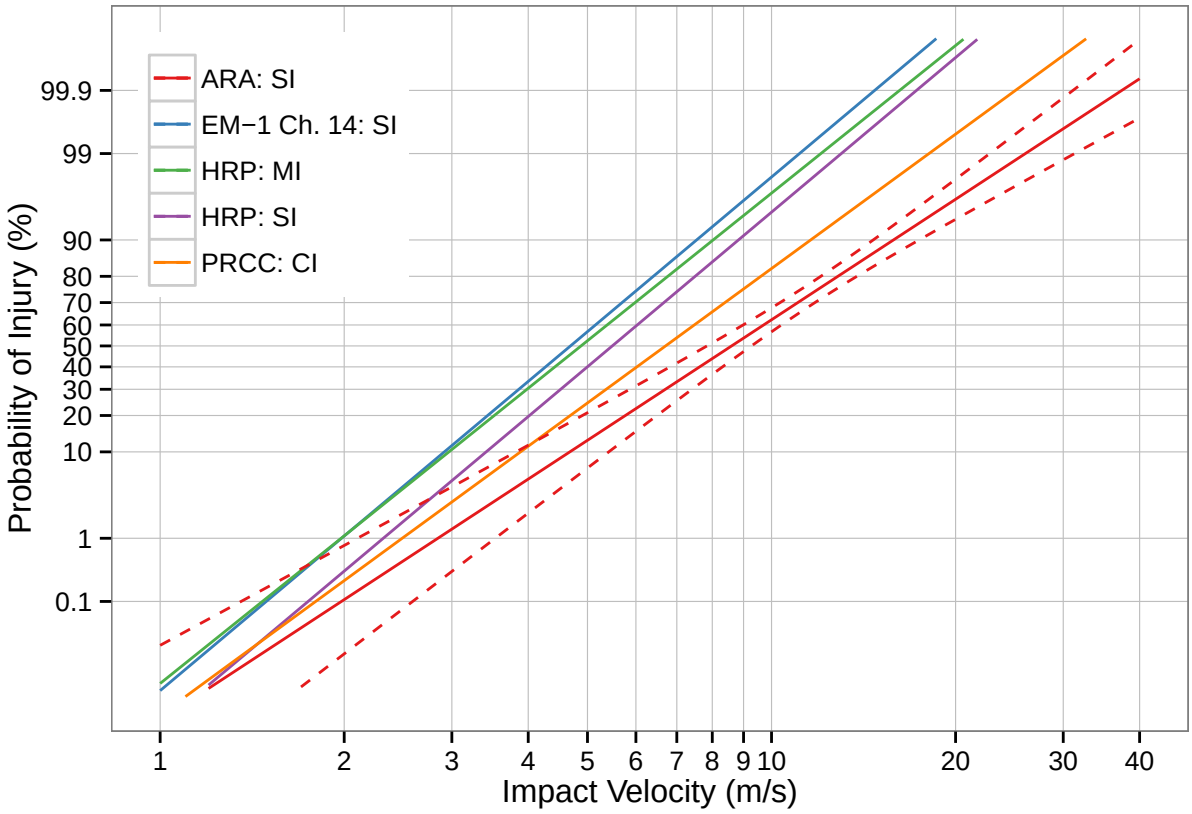

Figure 4.6: Probit models for SI, CI and MI due to perpendicular impact.

A comparison of the derived SI probit with existing SI and CI probit models is shown in Figure 4.6. The probit derived here has a larger V_{50} value than the other probit models, but a very similar slope. This results in greater SI predictions. The CI probit from PRCC is very similar to the derived probit, while the SI probit from EM-1 Ch. 14, which was derived using sheep data, is the least similar. Of the reviewed SI probits, the generated SI probit model is the only probit based entirely on human data. However, this probit was generated using digitized data. It is possible that there were overlapping data points which could not be distinguished and, therefore, were classified as only one subject.

We recommend the inclusion of the SI and FI probits generated here into HENRE 2.0. The FI probit was generated using data that provided detail on subject landing orientation. For SI, CI, and MI, the probit generated here is the only one based entirely on human data. Although probits for CI and MI exist, we recommended not including those injury levels. The CI probit was generated by assuming 1% mortality corresponded to 50% CI (Department of the Army 2013), and no source documentation or description of the MI probit generation process is available (Mercier 2001).

4.5 Penetrating Debris

Both EM-1 Ch. 14 and the PRCC report discuss blast injuries caused by penetrating debris. Developing injury criteria for penetrating debris is challenging because the likelihood of injury is dependent on several factors including the missile impacting area, shape, density, and velocity. Furthermore, in order to relate blast to penetrating injury, it is necessary to predict the particle shape and velocity distribution that an individual will be subjected to. A summary of the existing probit models and models generated here is given in Table 4.9. Each of these probits will be discussed here.

4.5.1 EM-1 Ch. 14/PRCC

Here, we are first interested in examining existing probit models in EM-1 Ch. 14 and the PRCC report which relate the likelihood of penetration to missile characteristics. Both documents discuss penetration injury caused by glass and non-glass objects. EM-1 Ch. 14

Table 4.9: Probit models for injury due to missile penetration.

Injury Level	Source	Probit Equation	Data/Assumptions
SI (glass)	ARA	$2.85\log_{10}(\frac{m^{0.5}v^2}{2F_{50}})$ $F_{50} = 89.45\frac{\mathrm{kg}^{0.5}\mathrm{m}^2}{\mathrm{s}^2}$	Based on canine data (Bowen et al. 1956). Assumes the likelihood of SI equals the likelihood that a glass shard will penetrate the abdominal wall.
MI (glass)	ARA	$2.85\log_{10}(\frac{m^{0.5}v^2}{2F_{50}})$ $F_{50} = 44.93\frac{\mathrm{kg}^{0.5}\mathrm{m}^2}{\mathrm{s}^2}$	Based on canine data (Bowen et al. 1956). Assumes the likelihood of MI equals the likelihood that a glass shard will penetrate the skin.
MI (stone)	ARA	$2.85\log_{10}(\frac{m^{0.5}v^2}{2F_{50}})$ $F_{50} = 178.5\frac{\mathrm{kg}^{0.5}\mathrm{m}^2}{\mathrm{s}^2}$	Based on goat/human data (Sperrazza et al. 1967). Assumes the probit slope is equal to the probit slope of the glass penetration probit and the likelihood of MI equals the likelihood that a glass shard will penetrate the skin.
CI (glass)	PRCC (Department of the Army 2013)	$9.1\log_{10}(\frac{v}{V_{50}})$ $V_{50} = 128\frac{\mathrm{m}}{\mathrm{s}}$ for 0.1g $V_{50} = 75\frac{\mathrm{m}}{\mathrm{s}}$ for 1.0g $V_{50} = 58\frac{\mathrm{m}}{\mathrm{s}}$ for 10g	Based on canine data (Bowen et al. 1956). Assumes the likelihood of CI equals the likelihood a glass shard will penetrate the abdomen. We were unable to reproduce this probit using the source data.
CI (stone)	PRCC (Department of the Army 2013)	$9.1\log_{10}(\frac{v}{V_{50}})$ $V_{50} = 188\frac{\mathrm{m}}{\mathrm{s}}$ for 0.1g $V_{50} = 104\frac{\mathrm{m}}{\mathrm{s}}$ for 1.0g $V_{50} = 61\frac{\mathrm{m}}{\mathrm{s}}$ for 10g	Based on goat/human data (Sperrazza et al. 1967). Assumes the probit slope is equal to the probit slope of the glass penetration probit and the likelihood of CI equals the likelihood stone will penetrate the skin. We were unable to reproduce this probit using the source data.

Table 4.10: The 50% penetration velocities of steel and stone.

Missile	Stone Mass (grams)	Ballistic limits Bare Skin	Military Uniform
Steel sphere*	1.0	60 m/s (197 ft/s)	154 m/s (505 ft/s)
	2.0	52 m/s (171 ft/s)	137 m/s (450 ft/s)
	10	40 m/s (131 ft/s)	111 m/s (364 ft/s)
Stone**	0.1	188 m/s (617 ft/s)	408 m/s (1340 ft/s)
	1.0	104 m/s (340 ft/s)	354 m/s (1160 ft/s)
	10	61.0 m/s (200 ft/s)	171 m/s (560 ft/s)

*Values obtained from Sperrazza et al. 1967.
**Values obtained from Department of the Army 2013.

discusses a British study which examined the effect of fragment shape on penetration velocity for a 53 mg missile (UK Ministry of Defense 1969)[6]. It was found that particles shaped as spheres required a lower velocity than randomly shaped fragments for penetration. Although providing useful qualitative information, the missile sizes and velocities explored in this study were deemed irrelevant for nuclear effects data (Reeves 2015).

A second study, discussed by both EM-1 Ch. 14 and the PRCC report, calculated the ballistic limits of isolated goat and human skin exposed to steel fragments weighing up to 15 g (Sperrazza et al. 1967). This study provides the following relationship between the ballistic limit (V_{50}) and the fragment mass

$$V_{50} = K\frac{a}{m} + b \tag{37}$$

where for skin $K = 1.2471 \cdot 10^6$ g/(m s), $b = 22.03$ m/s, a is the cross sectional area of the object, and m is the mass. For military uniforms, $K = 2.6107 \cdot 10^6$ g/(m s) and $b = 73.51$ m/s. The ballistic limits for 1.0, 2.0, and 10 g steel spheres are given in Table 4.10. These values correspond to a steel density of 8 gm/cm^3. In order to calculate the ballistic limits for stone, the PRCC report uses Equation 37 and assumes the drag coefficient of the stones is 1.0. Thus, the value of a/m is equal to the acceleration coefficients of the stones which were previously determined (Department of the Army 2013). Table 4.10 provides the resulting ballistic limits for stones[7].

EM-1 Ch. 14 does not provide a probit slope for stone or steel penetration, while the PRCC report assumes the stone penetration probit slope is equivalent to the glass penetration probit slope. Based on the digitization of Figure D-24 from the PRCC report this slope is approximately 9.4.

For glass penetration, the PRCC report and EM-1 Ch. 14 reference a study on glass abdominal penetration in dogs (Bowen et al. 1956). EM-1 Ch. 14 reports on another, more complex, study which examined the effects of penetration angle, fragment mass and impact velocity on V_{50} (Fletcher et al. 1980). In this study, experiments were performed in which

[6]EM-1 Ch. 14 states the missiles were 58 mg, while the UK source document states they were 53 mg.
[7]These values were pulled directly from the PRCC 2013 report; however, we were unable to reproduce these values precisely given the acceleration coefficients provided by the PRCC report.

Table 4.11: Glass impact velocities required for abdominal penetration in dogs.

Mass (g)	Velocity (m/s) 1% Penetration	50% Penetration	99% Penetration
0.1	75.0	134	232
1.0	44.0	76.0	131
10	30.7	53.0	91.5

Data derived from Bowen et al. 1956.

animals were placed in front of windows and exposed to overpressure waves. However, no probit curves were derived from this study.

The PRCC report provides a probit curve based on the canine abdominal penetration study (Bowen et al. 1956). In the penetration study, the threshold velocity for abdominal penetration is given as

$$\log_{10}(m) = -2.3054 + \frac{100.28}{v_0} \tag{38}$$

or

$$\log_{10}\left(\frac{m}{m_0}\right) = \frac{100.28}{v_0} \tag{39}$$

where m is mass of the missile in grams and v_0 is the threshold velocity in m/s. For this equation to be valid, m must be greater than m_0 ($m_0 = 0.00495$ g). The relationship between missile velocity v and probability of injury P is given as

$$\log_{10}(\frac{v}{v_0}) = 0.4842P. \tag{40}$$

Table 4.11 provides the calculated velocities required to result in 1%, 50% and 99% abdominal penetration. This table does not precisely agree with the Table D-15 from the PRCC report or Table 14A-15 from EM-1 Ch. 14, even though both were derived using the same study (Bowen et al. 1956). The PRCC report presents a probit model determined with data from this table. However, since we were unable to reproduce the table, we were also unable to reproduce the probit parameters.

4.5.2 Probit Generation

In this section, we derive new penetration injury probits for stone and glass because (1) we were unable to reproduce the glass penetration probit developed in the PRCC report and (2) we wanted to generate a probit for a continuous range of object masses. The PRCC report generated three separate probits for 0.1 g, 1.0 g, and 10 g. Instead, our aim is to include the mass in the probit equation. It was determined that the probit model for penetration should be of the following form:

$$\Phi^{-1}(p) = \beta \log_{10}\left(\frac{1}{2}\frac{m^a v^2}{F_{50}}\right) \tag{41}$$

The function given by Equation 41 was chosen because penetration is dependent on the kinetic energy of the missile ($\frac{1}{2}mv^2$). However, the penetration surface area likely increases

with the mass, causing the needed energy for penetration to increase. According to Equation 41, the needed impact energy for 50% penetration is $F_{50}m^{1-a}$. Thus, the value for a should be less than 1 (i.e., as mass increases, the energy needed for penetration increases).

To determine the value for a in the stone penetration model, we used the previously reported ballistic limit data for stone penetration of skin (Table 4.10). Since the stone data is for 50% penetration, Equation 41 can be reduced to

$$F_{50} = \frac{1}{2}m^a v^2 \tag{42}$$

Least squares regression of Equation 42 to the data in Table 4.10 resulted in an a value equal to 0.5 and an F_{50} value of 178.5 m^2/s^2 $kg^{1/2}$. Thus, the following equation defines the stone penetration probit model

$$\Phi^{-1} = \beta \log_{10}\left(\frac{1}{2}\frac{m^{0.5}v^2}{F_{50}}\right) \tag{43}$$

where β will be determined by assuming the same slope as the glass penetration probit.

To develop probits for glass penetration, data on skin and abdominal penetration in dogs were used (Bowen et al. 1956). To avoid the possibility that the abdominal penetration probability is ever greater than the skin penetration probability, the probit slopes for the skin and abdominal penetration models were set equal to each other, and the models were optimized using least squares regression. a was originally included in the model optimization, and it was found that the value was approximately equal to 0.5. To keep the probits consistent, the value of a was set to 0.5 and the model was re-optimized. The final glass penetration probits compared with data are shown in Figure 4.7.

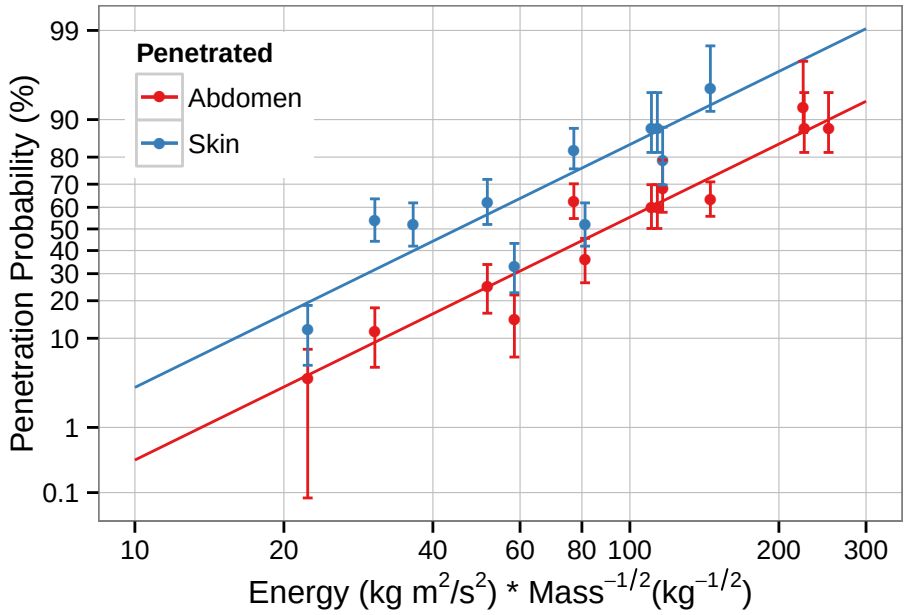

Figure 4.7: Probit model for glass penetration of skin and abdomen. Data obtained from a study in dogs (Bowen et al. 1956).

In finalizing the stone penetration probit, we assumed the slope was equal to that of the glass penetration probit, the same assumption that was used in the PRCC report. Thus, the stone penetration probit is:

$$2.85 \log_{10} \left(\frac{1}{2} \frac{m^{0.5} v^2}{2F_{50}} \right) \tag{44}$$

where $F_{50} = 178.5$ m^2/s^2 kg$^{1/2}$.

These probits provide information on the likelihood of penetration but do not relate that to injury. The PRCC report assumes 50% penetration corresponds to 50% CI; however, there are more mechanistic ways to relate penetration likelihood to injury. This would involve incorporating environmental information on the mass and number of missiles a person would encounter, and determining the probability of penetration that leads to a specified injury level. This is a needed step which will be discussed more in Section 6. For now, we use the same assumption as the PRCC report and equate the probability of skin and abdominal penetration to the probability of MI and SI, respectively.

4.5.3 Analysis

A comparison of the new probits with existing probits is shown in Figure 4.8. For this

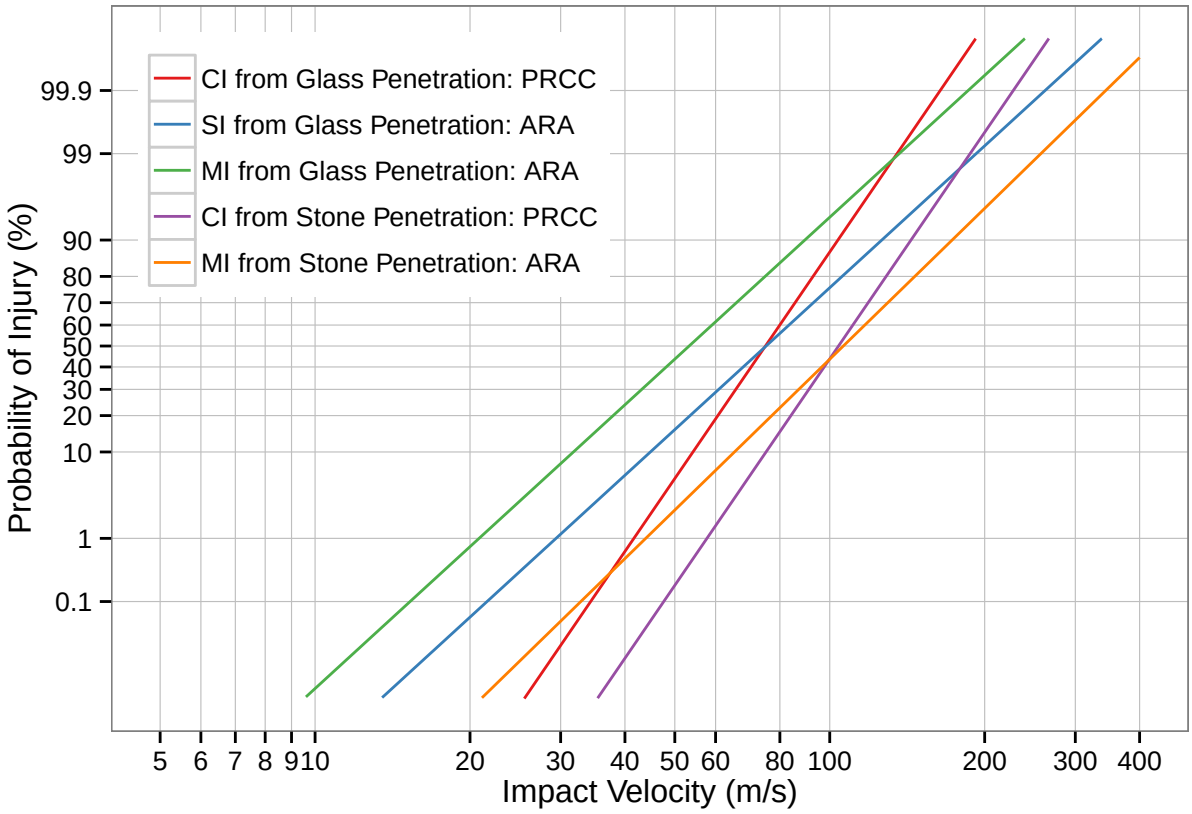

Figure 4.8: Comparing penetration probits for 1.0 gram missiles.

comparison, the mass of the missile is set to 1.0 g. To compare the probits generated here to preexisting ones, we rearranged Equation 43 to obtain:

$$\Phi^{-1} = 2\beta \log_{10}\left(\frac{v}{V_{50}}\right) \tag{45}$$

where

$$V_{50} = \sqrt{\frac{2F_{50}}{m^{0.5}}} \tag{46}$$

Because our models were derived with the same data as the PRCC probit models, we would expect them to be quite similar. This is indeed the case. The V_{50} from the MI stone penetration model generated here is equivalent to the V_{50} from the CI stone penetration model generated in the PRCC report. Similarly the V_{50} from the SI glass penetration model is equivalent to the V_{50} from the CI glass penetration model generated by PRCC. The main difference lies in the injury severity classification. We recommend the inclusion of the re-derived probits into HENRE 2.0.

4.6 Blunt Trauma

Blunt trauma occurs when a person is struck by an object which has sufficient kinetic energy to cause injury without penetration. Like other injuries, the effects of blunt trauma are highly dependent on the region of the body that is struck; the head, abdomen, and thorax are the most sensitive.

The PRCC report presents a probit relating the impact energy of an object to the likelihood of blunt trauma induced CI. This probit is based on data from a study done by the British during the Second World War (Zuckerman et al. 1944)[8]. In this study, lumps of hard crater debris and softer lumps of clay were impacted against small animals and dried human skulls. Injury was recorded if death, unconsciousness, major bone fracture, or severe rupture or hemorrhage occurred. Thus, although the PRCC report used this data to define CI, it is representative of SI as well.

The probit provided in Figure D-26 of the PRCC report was digitized to obtain the following equation:

$$\Phi^{-1}(p) = 2.51 \log\left(\frac{E}{E_{50}}\right) \tag{47}$$

where E is the energy of the missile and $E_{50} = 67.37$ J. EM-1 Ch. 14 uses the probit model developed in the PRCC report to provide V_{50} values of 17.4, 7.6, and 5.5 m/s for missile weights of 0.45, 2.3, and 4.5 kg which agrees with the E_{50} value derived through digitization. We did not seek to generate a new probit for blunt trauma. We recommend including the probit given by Equation 47 into HENRE 2.0I, with the aim of eventually replacing it with a more sophisticated model.

[8] We were unable to obtain this original source. The information provided here was given by Drake et al. 1978.

5 Summary

This work outlines a translation model linked with velocity probit models that predict the probability of injury following complex blast wave exposures. These models can be linked with nuclear environment tools that predict blast parameters in urban areas to estimate the potential fatalities and casualties due to blast.

5.1 Translation Models

The translation model requires the following inputs: the dynamic pressure wave, the time-course of the wind velocity, and the acceleration coefficient of the object of interest. The acceleration coefficient is a function of the object's mass, area presented to the wind, and drag coefficient. With these inputs, the model calculates the translational profile (i.e., distance, velocity, and acceleration) as a function of time. This is an update to existing methods because complex blast waves can be directly inputted to determine an object's velocity.

5.2 Finalized Injury Criteria Models for Inclusion in HENRE 2.0

Table 5.1 provides a summary of all probit models recommended for inclusion into HENRE 2.0. For tertiary injury, these include probits for FI and SI, and for secondary injury, these include probits for SI and MI. These recommendations are based on a thorough review of the existing injury criteria models used by the nuclear effects community.

For both FI and SI due to decelerative tumbling, multiple injury criteria models exist. These include previously generated probits presented in EM-1 Ch 14 and by Dr. Mercier at

Table 5.1: Summary of probit models recommended for inclusion in HENRE 2.0

	Fatal Injury	**Serious Injury**	**Moderate Injury**
Decelerative Tumbling (Urban Environment)	if $v \leq 46.01$ m/s: $2.86\log_{10}(\frac{v}{V_{50}})$; $V_{50} = 40.19\frac{\text{m}}{\text{s}}$ if $v > 46.01$ m/s: $19.55\log_{10}(\frac{v}{V_{50}})$; $V_{50} = 45.11\frac{\text{m}}{\text{s}}$	if $v \leq 32.37$ m/s: $2.40\log_{10}(\frac{v}{V_{50}})$; $V_{50} = 9.22\frac{\text{m}}{\text{s}}$ if $v > 32.37$ m/s: $6.42\log_{10}(\frac{v}{V_{50}})$; $V_{50} = 20.24\frac{\text{m}}{\text{s}}$	None
Decelerative Tumbling (Open Field)	$19.55\log_{10}(\frac{v}{V_{50}})$; $V_{50} = 45.11\frac{\text{m}}{\text{s}}$	$6.42\log_{10}(\frac{v}{V_{50}})$; $V_{50} = 20.24\frac{\text{m}}{\text{s}}$	None
Perpendicular Impact	$7.19\log_{10}(\frac{v}{V_{50}})$; $V_{50} = 15.35\frac{\text{m}}{\text{s}}$	$4.84\log_{10}(\frac{v}{V_{50}})$; $V_{50} = 8.61\frac{\text{m}}{\text{s}}$	None
Glass Penetration	None	$2.85\log_{10}(\frac{m^{0.5}v^2}{2F_{50}})$; $F_{50} = 89.45\frac{\text{kg}^{0.5}\text{m}^2}{\text{s}^2}$	$2.85\log_{10}(\frac{m^{0.5}v^2}{2F_{50}})$; $F_{50} = 44.93\frac{\text{kg}^{0.5}\text{m}^2}{\text{s}^2}$
Stone Penetration	None	None	$2.85\log_{10}(\frac{m^{0.5}v^2}{2F_{50}})$; $F_{50} = 178.5\frac{\text{kg}^{0.5}\text{m}^2}{\text{s}^2}$
Blunt Trauma	None	$2.51\log_{10}(\frac{E}{E_{50}})$; $E_{50} = 67.37\text{J}$	None

the HRP (Reeves 2015; Mercier 2001) and probits developed here using motorcycle accident data (Hurt et al. 1981a). Previously generated models are based on unobtainable data and/or the model generation process was unclear. The motorcycle accident data provides a more verifiable and accurate representation of injury probabilities that might be observed in an urban environment. Thus, we recommend the inclusion of the probits derived using motorcycle data into HENRE 2.0 to predict injury in urban environments at low velocities. For injury predictions in open field environments, the probits given by EM-1 Ch. 14 and presented by Dr. Mercier are very similar. However, more description was given by EM-1 Ch. 14 on probit generation and, thus, the probits from EM-1 Ch. 14 are recommended for inclusion into HENRE 2.0 to predict decelerative tumbling injuries in open field environments as well as injuries in urban environments at high velocities (Reeves 2015).

For CI and MI due to decelerative tumbling, we did not generate new probits. The existing CI model for decelerative tumbling is based on one data point from a goat study in which all of the injured goats died (Anderson et al. 1961). Furthermore, the slope was assumed to equal that of the perpendicular impact model developed by PRCC. The source data and derivation of the MI model is not described and warrants further investigation. For these reasons, we do not recommend the inclusion of a CI or MI model at this time.

For both FI and SI due to perpendicular impact with a non-yielding surface, multiple probits exist. These include preexisting probits (Department of the Army 2013; Drake et al. 1993; Mercier 2001) and probits generated here using data from human free fall studies (Lapostolle et al. 2005; Beale et al. 2000; Dickinson et al. 2012). These probits were derived using sheep data, human data, or a combination of the two. Due to assumptions required to translate from sheep to humans, we recommend including a model that is based solely on human data. For FI, these include the models derived in PRCC report and by us using human free fall studies. Because the FI probit generated here used a study that contained more detailed information on falling dynamics, we recommend the inclusion of this probit into HENRE 2.0. For SI, the probit generated by us is the only one based on human data, and therefore, we recommend the inclusion of this probit.

Probits also exist for CI and MI due to perpendicular impact. The MI probit is poorly documented, with no the source data description (Mercier 2001). The CI probit was derived by assuming 1% mortality corresponds to 50% CI (Department of the Army 2013). Due to the underlying assumptions and lack of documentation, we do not recommend inclusion of the CI or MI probits.

Secondary injury criteria models are available for CI, SI, and MI. The only preexisting penetration injury criteria models were found in the PRCC report; however, we were unable to re-derive the stone or glass penetration probit using the source data. Here, we developed new probits, using the same source data as the PRCC report, that include the mass of the object in the probit equation. We assumed that the likelihood of a missile penetrating the skin was equivalent to MI and the likelihood of a missile penetrating the abdomen was equivalent to SI. Because the source data used by the PRCC report did not contain data on the likelihood of stone penetrating the abdomen, no SI model for stone exists.

Finally, for blunt trauma, only a probit model for SI exists. We were unable to obtain the source documentation for this blunt trauma model (Zuckerman et al. 1944). This probit is based on data obtained by performing impact studies with small animals and dried human skulls (Drake et al. 1978). We propose the inclusion of this blunt impact model into

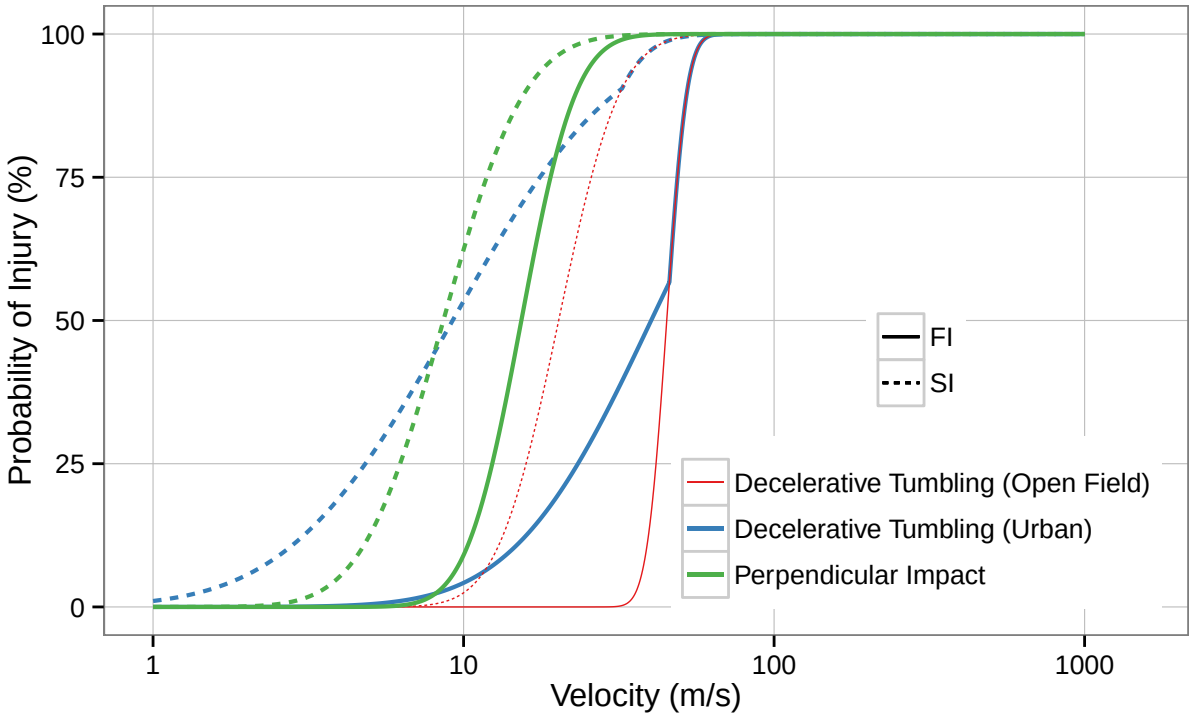

Figure 5.1: Final tertiary injury probit models.

HENRE 2.0 so that a complete picture of injury types is implemented. In the future, more sophisticated models of blunt injury should be explored.

Figure 5.1 compares the tertiary probit models recommended for implementation in HENRE 2.0. The models for SI and FI predict that, at low velocities, injuries due to decelerative tumbling in urban environments are more likely than injuries due to perpendicular impact. In decelerative tumbling, multiple impacts occur, which could lead to an increased likelihood of a head injury when compared with perpendicular impact (Drake et al. 1978). Also, although the generated models improve upon the existing probits, further model development may be warranted. Work could be done to improve the probit model structure and/or underlying data. In addition to impact velocity, other metrics, such as age and orientation, are used elsewhere to predict mortality (Dickinson et al. 2012; Lapostolle et al. 2005). These models could be explored to see if they provide a more accurate representation of the data.

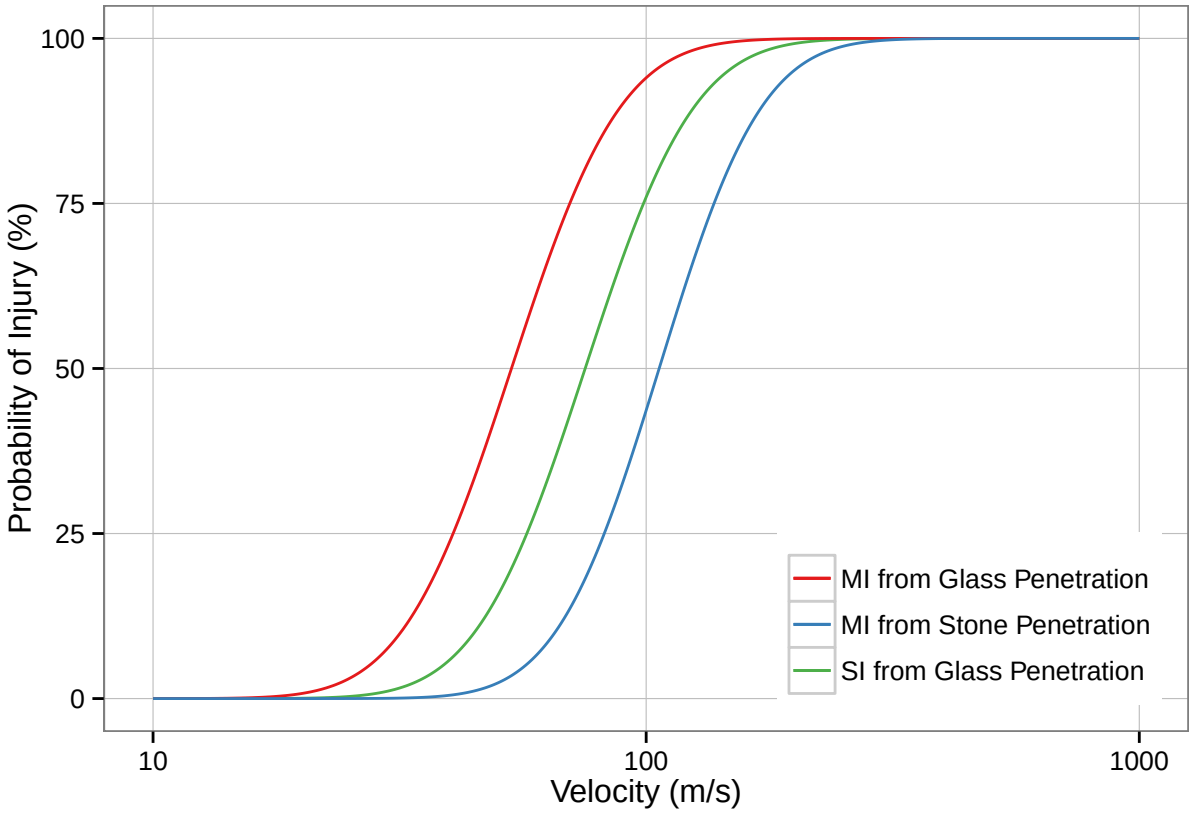

Figure 5.2: Final penetration injury probit models for 1.0 gram missiles.

The penetrating injury probits for stone and glass with masses of 1.0 g are shown in Figure 5.2. Given the same missile mass and velocity, the likelihood of MI and SI from glass penetration is greater than the likelihood of SI from stone penetration. These models assume that the probability of SI and MI are equivalent to the probability of abdominal and skin penetration, respectively. However, it is possible that a stone penetration of the skin is actually more severe than a glass shard penetration due to a larger impact area.

6 Conclusions and Future Work

This work provides an incremental improvement to blast injury calculations; however, there are several facets of the modeling techniques discussed that can be improved upon in the future.

Future work to improve the translation model should involve refining the deceleration portion of the model and incorporating directional components for the wind velocity and dynamic pressure. Contemporary work has been done to estimate the distance traveled by a pedestrian who has been hit by a vehicle. Models have been developed which predict the distance a pedestrian is thrown based on the vault angle and impact speed (Evans et al. 1999). These models can be used to assess or replace the deceleration portion of the translation model reviewed here. As for adding directional components, the translation model currently assumes the direction of the dynamic wave is constant, but in urban environments this is likely not the case. Thus, future work should involve representing the blast wave and translational profile using vector notation.

Probit models for FI and SI due to decelerative tumbling and perpendicular impact have been generated using data obtained from human accidents. To obtain more precise probits, a more thorough epidemiological analysis needs to be performed. For example, in generating the decelerative tumbling probit, we used data from a study on motorcycle accidents. This study grouped together subjects who did or did not have helmets and had different types of motion following the crash. An ideal analysis would involve using the raw data from this study to select subjects with specific criteria (e.g., only include subjects whose injuries were due to tumbling). A similar analysis could be done with data on free fall victims. This would result in probits which are based on the most appropriate data for representing the injuries observed following blast waves in urban environments.

Probit models were developed for SI and MI due to penetrating injuries. These models provide the likelihood that a given fragment will penetrate the skin or abdomen. However, relating fragment penetration to injury has not yet been done. Future work will involve determining this relationship either by using past work or by developing new models. The Operational Requirement-based Casualty Assessment (ORCA) software package contains models which track penetrating fragments and determine the likelihood of injury caused by the fragment based on the region of the body penetrated. In turn, the likelihood of injury due to multiple fragments can be ascertained.

For glass penetration, more detailed models which relate the shattering of a window to injury probability have been generated. These include a Shard Fly-Out Model (SFOM) and the Multi-Hit Glass Penetration (MHGP) Model (Meyer et al. 2004). The SFOM determines if and how a window breaks following a blast wave and generates a distribution of glass shards with details on the shape, mass, velocity, and orientation of each shard. This model includes details on the window type and thickness. The MHGP Model, in turn, determines whether injury occurs based on the glass shards which come into contact with an individual. The injury criteria is based on the depth of penetration of glass shards which is given by

$$x_{max} = \frac{m}{0.1605 A_p} \ln(1 + 0.001216V) \tag{48}$$

where x_{max} is the maximum depth of penetration in cm, m is the mass in g, A_p is the

presented area in cm^2, V is the striking velocity of a shard in m/s (Weber et al. 2012). Based on criteria set forth in Weber et al. 2012, a fragment that penetrates 1 to 12 mm causes mild injury, and a fragment that penetrates more than 12 mm causes serious injury. Going forward, we must determine how best to integrate the information from more advanced models into HENRE for casualty estimation.

We have not addressed a revision of blunt injury models here. However, work has been done correlating blunt trauma to specific body parts with injury. For example, White et al. measured blunt trauma to the head due to a 10-lb missile as a function of impact velocity (White et al. 1965). Furthermore, another group at ARA has developed Massive Projective/Whole Body Displacement software which simulates collisions between the human body and large rigid objects to predict the risk of injury due to blunt impact (Walilko et al. 2014). This software uses mechanical principles to model collisions to different parts of the body. Future work may involve incorporating this software into HENRE.

In conclusion, the models presented here provide an incremental improvement to blast injury calculations and facilitate injury prediction in urban environments. By combining the translation and probit models, the probability of injury and mortality can be predicted for an individual exposed to complex nuclear blast waves. As discussed above, a number of other improvements could be undertaken in the future.

7 References

Anderson, R. S., Stemler, F. W., and Rogers, E. B., 1961. *Air Blast Studies with Animals II*. DASA-1193, U.S. Army, Chemical Research and Development Laboratories, Army Chemical Center, Maryland.

Baker, S. P., O'Neill, B., Haddon, W., and Long, W. B., 1974. "The injury severity score: a method for describing patients with multiple injuries and evaluating emergency care," *The Journal of Trauma*, 14(3), 187–96.

Beale, J. P., Wyatt, J. P., Beard, D., Busuttil, A., and Graham, C. A., 2000. "A five year study of high falls in Edinburgh," *Injury*, 31(7), 503–8.

Bowen, I. G., Fletcher, E. R., Richmond, D. R., Hirsch, F. G., and White, C. S., 1968. "Biophysical mechanisms and scaling procedures applicable in assessing responses of the thorax energized by air-blast overpressures or by nonpenetrating missiles," *Annals of the New York Academy of Sciences*, 152(1), 122–46.

Bowen, I. G., Albright, R. W., Fletcher, E. R., and White, C. S., 1961. *A Model Designed to Predict the Motion of Objects Translated by Classial Blast Waves*. CEX-58.9, Lovelace Foundation for Medical Education and Research, Albuquerque, New Mexico.

Bowen, I. G., Richmond, D. R., Wetherbe, M. B., and White, C. S., 1956. *Biological Effects of Blast from Bombs. Glass Fragments as Penetrating Missiles and Some of the Biological Implications of Glass Fragmented by Atomic Explosions*. AECU-3350, Lovelace Foundation for Medical Education and Research, Albuquerque, New Mexico.

Department of the Army, 2013. *Personnel Risk and Casualty Criteria for Nuclear Weapons Effects*. DA PAM 50-7, Washington, D.C.

Dickinson, A., Roberts, M., Kumar, A., Weaver, A., and Lockey, D. J., 2012. "Falls from height: injury and mortality," *Journal of the Royal Army Medical Corps*, 158(2), 123–7.

Drake, M. K., Fricke, M. P., Groce, D. E., Kaul, D. C., Rindfleisch, C. J., Swenson, J. B., and Woolson, W. A., 1978. *An Interim Report of Collateral Damage*. DNA 4734Z, Science Applications, Inc., Lajolla, California.

Drake, M., and Woolson, W., 1993. "Chapter 14-Effects on Personnel," *Effects Manual-1: Capabilities of Nuclear Weapons*. Alexandria. Defense Nuclear Agency.

Evans, A. K., and Smith, R., 1999. "Vehicle speed calculation from pedestrian throw distance," *Proceedings of the Institution of Mechanical Engineers, Part D: Journal of Automobile Engineering*, 213(5), 441–7.

Fletcher, E. R., and Bowen, I. G., 1966. *Blast-Induced Translational Effects*. DASA 1859, Lovelace Foundation for Medical Education and Research, Albuquerque, New Mexico.

Fletcher, E. R., Yelverton, J. T., Hutton, R. A., and Richmond, D. R., 1975. *Probability of Injury from Airblast Displacement as a Function of Yield and Range*. DNA 3779T, Lovelace Foundation for Medical Education and Research, Albuquerque, New Mexico.

Fletcher, E. R., Richmond, D. R., and Yelverton, J. T., 1980. *Glass Fragment Hazard from Windows Broken by Airblast*. DNA 5593T, Lovelace Biomedical and Environmental Research Institute, Albuquerque, NM.

Hague, D. J., 2001. "Calculation of impact speed from pedestrian slide distance," *The Institute of Traffic Accident Investigators. Proceedings of the 5th Interantional Conference: 17th and 18th November, 2001*, 101–8.

Hurt, H. H., Ouellet, J. V., and Thom, D. R., 1981a. *Volume I: Techinical Report. Motorcycle Accident Cause and Factors Identification of Countermeasures*. Traffic Safety Center, University of Southern California, Los Angeles, CA.

Hurt, H. H., Ouellet, J. V., and Thom, D. R., 1981b. *Volume II: Appendix/Supplemental Data. Motorcycle Accident Cause and Factors Identification of Countermeasures*. Traffic Safety Center, University of Southern California, Los Angeles, CA.

Jackson, M., and Wright, S. C., 2013. *PDCALC 8.1 Personnel Vulnerability Tables Update*. U.S. Army Nuclear & CWMD Agency and Science Applications International Corporation.

Lapostolle, F., Gere, C., Borron, S. W., Pétrovic, T., Dallemagne, F., Beruben, A., Lapandry, C., and Adnet, F., 2005. "Prognostic factors in victims of falls from height," *Critical Care Medicine*, 33(6), 1239–42.

Lewis, W. S., Lee, A. B., and Grantham, S. A., 1965. "Jumpers syndrome. The trauma of high free fall as seen at Harlem Hospital," *The Journal of Trauma*, 5(6), 812–8.

Mercier, J. R., 2001. "Human Response Criteria for Blast Effects," *Presentation at the Deffense Threat Reduction Agency Human Response Panel Meeting, October 9th, 2001 (Unpublished Data)*,

Meyer, S., Little, L., and Conrath, E., 2004. *Injury Based Glass Hazard Assessment*. Applied Research Associates, San Antonio, Texas.

NATO, 2009. *AMedP-8 (C) NATO Planning Guide for the Estimation of CBRN Casualties Study Draft 5*. November, National Atlantic Treaty Organization.

Needham, C. E., 2010. *Blast Waves*. Springer, Berlin, Heidelberg, 152.

Otte, D., 2001. "Importance of speed related traces on the scene for determination of collision speed in pedestrian and bicycle accidents," *The Institute of Traffic Accident Investigators. Proceedings of the 5th Interantional Conference: 17th and 18th November, 2001*, 93–9.

R Core Team, 2014. *R: A Language and Environment for Statistical Computing*. R Foundation for Statistical Computing, Vienna, Austria.

Reeves, G. I., 2015. "Chapter 14-Effects on Personnel, Revision 1," *Effects Manual-1: Capabilities of Nuclear Weapons*. DTRA-EM-1-CH14 (R1). Fort Belvoir, VA.

Richmond, D. R., Fletcher, E. R., Jones, R. K., and Jackson, W. S., 1974a. *Airblast Effects Inside Field Fortifications. Middle North Series Mixed Company III Event*. POR 6622-1, Lovelace Foundation for Medical Education and Research, Albuquerque, New Mexico.

Richmond, D. R., and Jackson, W. S., 1974b. *Airblast Effects in Foxholes. Middle North Series Mixed Company III Event*. POR 6622-2, Lovelace Foundation for Medical Education and Research, Albuquerque, New Mexico.

Shapiro, A. H., 1954. "Analysis of Moving Shocks," *The Dynamics and Thermodynamics of Compressible Fluid Flow - Volume 2*. The Ronald Press Company, 1000–7.

Soetaert, K., and Petzoldt, T., 2010a. "Inverse modelling, sensitivity and Monte Carlo analysis in R using package FME," *Journal of Statistical Software*, 33(3), 1–28.

Soetaert, K., Petzoldt, T., and Setzer, R. W., 2010b. "Solving differential equations in R: Package deSolve," *Journal of Statistical Software*, 33(9), 1–25.

Sperrazza, J., and Kokinakis, W., 1967. *Ballistic Limits of Tissue and Clothing*. BRL-TN-1645, Army Ballistic Research Lab, Aberden Proving Ground, MD.

UK Ministry of Defense, 1969. "Chapter 12-Vulnerability of human targets to fragmenting and blast weapons," *Textbook of Air Armament Part 2 (Target Vulnerability and Weapon Effectiveness)*. Air Publication 110A-0300-1B12.

Venables, W. N., and Ripley, B. D., 2002. *Modern Applied Statistics with S*. Springer, New York.

Walilko, T. J., Weiss, G., and Forman, J., 2014. *Massive Projectile/Whole Body Displacement Software Program*. Applied Research Associates, Inc.

Weber, P., and Millage, K., 2012. *NREG Current Glass Injury Status*. ARA/HS-TN-12-007-A, Applied Research Associates, Inc., Arlington, Virginia.

White, C. S., Bowen, I. G., and Richmond, D. R., 1965. *Biological Tolerance to Air Blast and Related Biomedical Criteria*. CEX-65.4, Lovelace Foundation for Medical Education and Research, Albuquerque, New Mexico.

Zuckerman, S., Burns, B. D., and Black, P. M., 1944. *The Wounding Power of Debris*. Report R.C. 423, Ministry of Home Security, Oxford, England.

Appendix A R Code

A.1 Script for Running Models and Generating Output

The following R script was used to run the models given in Appendix A.2 and A.3. The script contains code which verifies the R implementation and performs validations. This code outputs the Figures given in Section 3. Some of these verifications and validations rely on input datasets, including the digitized version of Figure 2.2 from Bowen et al. 1961, Table 4.1 from Bowen et al. 1961, Figure A1 from Fletcher et al. 1975, Figure 4 from Otte 2001, and Figure 11.8 from Needham 2010.

```
#Script for implementing translation models discussed in DTRA-TR-14-23
#
#Jacqui Wentz
#jwentz@ara.com
#1/14/2015

# Set up ------------------------------------------------------------------
setwd("C:/Users/jwentz/Documents/Projects/NSF/Injury Criteria Modeling/")
library(deSolve)
library(ggplot2)
library(scales)
source("Scripts/objectVelocityBowen.R")
source("Scripts/objectVelocityWithDecelFletcherFinal.R")

#Conversions
psi_to_kpa <- 6.89475729  #Conversion factor to change from psi to kpa

#Determine ratio of overpressure duration to dynamic pressure duration (based
    on Figure 2.2 and Table 3.1 from Bowen 1961)
tratio_data_1 <- read.csv("Digitized//Bowen1961//Bowen1961_Figure2point2.csv")
tratio_data_1$tp_Over_tu <- 1/tratio_data_1$tu_Over_tp
tratio_data_2 <- data.frame(Ps=c(0.068,.10,.15,.20,.25,.30,.35,.4,
                                 .5,.6,.7,.8,1,1.3,1.7),
                            tp_Over_tu=c(.9,.885,.875,.855,.840,.835,.805,
                                         .793,.76,.74,.72,.71,.675,.635,.585))
tratio_data_2$tu_Over_tp <- 1/tratio_data_2$tp_Over_tu
tratio_data <- rbind(tratio_data_1,tratio_data_2)

#Load in functions
inverse <- function (f, lower=0, upper=10) {
  function (y) uniroot((function (x) f(x) - y), lower=lower, upper=upper)[1]
}
find_overpressure <- inverse(function (x) 2.5*x^2/(7+x)*(1+2*10^(-8)*x^4)/
    (1+10^(-8)*x^4), 0, 500)
find_decay_rate <- inverse(function (x) (exp(-x)+x-1)/x^2,-10,10)

# Verifying acceleration portion of translation model ---------------------

#Parameters obtained from Bowen 1961, Section 5.2
ps <- 5.3       #psi
p0 <- 13.3      #psi
tp_plus <- .964 #s
```

```
c0 <- 1120      #ft/s
alpha <- 0.03   #ft^2/lb

Ps <- ps/p0
tp_Over_tu <- approx(x=tratio_data$Ps,y=tratio_data$tp_Over_tu, xout=c(Ps))$y
tu_plus <- tp_plus/tp_Over_tu

A <- (alpha*144)*(p0*32.174049)*tu_plus/c0 #unitless
Vini <- c(V=0,D=0)
params <- c(Ps,A)
out <- ode(y = Vini, func = objectVelocityBowen, times = seq(0,1,.002), parms
    = params, method = "ode23")
max(out[,2])*c0
#Gives max veloctiy of 23.0 ft/s compared with value from paper of 23.4 ft/s

#Table 4.1 Verification
BowenTabData <- read.csv("Digitized/Bowen1961/Bowen1961Table4.1.csv")
Ps <- 0.1
modelData <- data.frame(P=c(),V=c(),D=c(),A=c())
maxVModel <- data.frame()
Vini <- c(V=0,D=0)
for (Ai in unique(BowenTabData$A)) {
  params <- c(Ps,Ai)
  out <- ode(y = Vini, func = objectVelocityBowen, times = seq(0,1,.002),
      parms=params, method = "ode23")
  minIndex <- min(which(out[,2] %in% max(out[,2])))
  out <- out[1:minIndex,]
  maxVModel <- rbind(maxVModel,data.frame(P=Ps,Vdata=max(subset(BowenTabData,A
      ==Ai)$V),V=out[minIndex,2],D=out[minIndex,3],A=Ai))
  modelData <- rbind(modelData,data.frame(P=Ps,V=out[,2],D=out[,3],A=Ai))
}

ggplot(data=BowenTabData) +
  geom_point(aes(D,V,color=factor(A)),size=2,shape=1) +
  geom_text(data=maxVModel,
            aes(D,V,
                label=paste("A=",A,"\nMax. Velocity (Model): ",round(V,5),
                            "\nMax. Velocity (Data): ",round(Vdata,5),sep=""),
                color=factor(A)),
            vjust=.5,hjust=-0.06,size=3) +
  geom_line(data=modelData,aes(D,V,color=factor(A))) +
  scale_x_continuous(limits=c(0,0.02)) +
  scale_y_continuous(limits=c(0,0.05)) +
  xlab("Distance (dimensionless)") +
  ylab("Velocity (dimensionless)") +
  scale_colour_brewer(palette="Set1") +
  theme_bw() +
  theme(text=element_text(size=12),
        legend.position="none",
        panel.grid.major=element_line(color="gray"),
        panel.grid.minor=element_blank())
#ggsave("Figures/BowenVerification_v7.pdf",width=6.5,height=5.5)
```

```
# Verifying Fletcher Report Run 10, 10kT ---------------------------------

#Baseline parameters
p0 <- 14.7*psi_to_kpa #kpa
c0 <- 340.29 #m/s
T0 <- 298 #K
R <- 287.058 #J/kg/K = m^2/s^2/K
g <- 7/5 #1; adiabatic index
m0 <- 75 #kg

#Blast wave/object parameters
W <- 10                     #kT; Given in Fletcher report
qs <- 14*psi_to_kpa         #kPa; Given in Fletcher report
ps <- 27.4*psi_to_kpa       #kPa; Given in Fletcher report
tp_plus <- 0.165*W^(1/3)    #s; Given in Fletcher report
tu_plus <- 0.312*W^(1/3)    #s; Given in Fletcher report
Ip <- 1.15*W^(1/3)*psi_to_kpa  #kPa s; Given in Fletcher report
Iq <- 0.474*W^(1/3)*psi_to_kpa #kPa s; Given in Fletcher report
m <- 75 #kg

#Dimensionless quantities
RBar <- R*T0/c0^2
Ps <- ps/p0
Qs <- qs/p0
M <- m/m0
#Acceleration coefficient for man initially prone with a random orientation
Dlim <- 1.79832/tu_plus/c0 #Distance at which acceleration coefficient is Amax
Amin <- .00286742601*(p0*1000)*tu_plus/c0
Amax <- .00614448431*(p0*1000)*tu_plus/c0
Achange <- tu_plus^3*c0*(p0*1000)/31.65^2 #Determines how A changes with D^2

#Deceleration
F1=8.9029*(.3048/c0)^.61692*tu_plus

#Find wave decay rates based on impulse and peak
n <- find_decay_rate(Ip/p0/tp_plus/Ps)$root
r <- find_decay_rate(Iq/p0/tu_plus/Qs)$root

#Run ODE
Vini <- c(V=0,D=0)
params <- c(Ps,Qs,n,r,tp_plus/tu_plus,M,RBar,Dlim,Amin,Amax,Achange,F1,g)
out <- ode(y = Vini, func = objectVelocityWithDecelFletcherFinal,
           times = seq(0,5,.002), parms = params, method="ode23")
modelData <- data.frame(time=out[,1]*tu_plus,velocity=out[,2]*c0,
                        distance=out[,3]*c0*tu_plus)

#Load in and set up verification data
Curve <- read.csv("Digitized/Fletcher1975/FigureA1Curve.csv")
TimePoints <- read.csv("Digitized//Fletcher1975//FigureA1TimePoints.csv")
TimePoints$label2 <- paste(factor(sprintf("%.2f",round(TimePoints$label,2))),"
    s",sep="")
modelTimePoints <- data.frame(time=c(),velcoity=c(),distance=c())
for (time in TimePoints$label) {
  modelTimePoints <- rbind(modelTimePoints,modelData[which(abs(modelData$time-
```

```
      time)==min(abs(modelData$time-time))),])
}

#Generate comparison plot between data and simulation
plot <- ggplot() +
  geom_line(data=Curve,aes(Distance.m,Velocity.mpers)) +
  geom_point(data=TimePoints,aes(Distance.m,Velocity.mpers),shape=1) +
  geom_text(data=subset(TimePoints,label2!="0.20 s"),
            aes(Distance.m,Velocity.mpers,label=label2),
            vjust=.1,hjust=-.2,size=3) +
  geom_text(data=subset(TimePoints,label2=="0.20 s"),
            aes(Distance.m,Velocity.mpers,label=label2),
            vjust=.2,hjust=1.2,size=3) +
  geom_line(data=modelData,aes(distance,velocity),color="red",size=.25) +
  geom_point(data=modelTimePoints,
             aes(distance,velocity),
             color="red",shape=1) +
  scale_x_continuous(limits=c(0,23)) +
  xlab("Distance Traveled (m)") +
  ylab("Velocity (m/s)") +
  theme_bw() +
  theme(text=element_text(size=12),
        panel.grid.major=element_line(color="gray"),
        panel.grid.minor=element_blank())
mergedTimePoints <- cbind(modelTimePoints,TimePoints)
for (i in 1:nrow(mergedTimePoints)) {
  row <- mergedTimePoints[i,]
  plot <- plot +
    geom_line(data=data.frame(velocity=c(row$velocity,row$Velocity.mpers),
                              distance=c(row$distance,row$Distance.m)),
              aes(distance,velocity),linetype=2)
}
plot
#ggsave("Figures/FletcherVerification_v7.pdf",width=6.5,height=4.5)

# Model validation using accident data from Otte2001 ----------------------

#Simulation parameters
c0 <- 340.29 #m/s
tu_plus <- 1 #Need to have value as place holder, doesn't affect results
F1 <- 8.9029*(.3048/c0)^.61692*tu_plus

#Run simulation for different initial velocities and store max distance
decelData <- data.frame(model=c(),calc=c())
for (vi in seq(1,30,1)) {
  V <- vi/c0
  Vini <- c(V=V,D=0)
  params <- c(0,0,1,1,1,1,RBar,0,0,0,0,F1,g) #Set blast wave params to zero
  out <- ode(y = Vini, func = objectVelocityWithDecelFletcherFinal,
             times = seq(0,10,.002), parms = params, method="ode23")
  modelData <- data.frame(time=out[,1]*tu_plus,velocity=out[,2]*c0,
                          distance=out[,3]*c0*tu_plus)
  decelData <- rbind(decelData,data.frame(vi=vi,model=max(modelData$distance),
                                          calc=10^(-1.15822+1.61692*log10(vi))
```

```
                                        ))
}

#Load in validation data
otteData <- read.csv("Digitized//Otte2001//Figure4.csv")

#Plot data against model predictions
ggplot(data=decelData,aes(vi,model)) +
  geom_line() +
  geom_point(data=otteData,aes(x*.28,Curve1),color="blue",shape=1) +
  xlab("Velocity (m/s)") +
  ylab("Distance (m)") +
  theme_bw() +
  theme(text=element_text(size=12),
        legend.position="none",
        panel.grid.major=element_line(color="gray"),
        panel.grid.minor=element_blank())
#ggsave("Figures/OtteDecelerationValidation_v7.pdf",width=6.5,height=4.5)

# Model Validation: Jeep Data (Needham2010) -------------------------------

#Load in validation data
jeepData <- read.csv("Digitized/Needham2010//Figure11point8.csv")

#Baseline parameters
T0 <- 298 #K
R <- 287.058 #J/kg/K = m^2/s^2/K
RBar <- R*T0/c0^2
g <- 7/5
p0 <- 14.7*psi_to_kpa #kPa
c0 <- 340.29 #m/s
m0 <- 75

#Object parameters
alpha <- .005 #m^2/kg; very rough approximation for a jeep
m <- 1000 #kg; approximate weight of jeep

#Dimensionless parameters (same for each simulation)
M <- m/m0
Dlim <- -1 #Set Dlim to less than one so that A is constant at Amax
Amin <- 0
Achange <- 0


#Iterate through dynamic impulses and run simulations under several conditions
    . Store max and min for each dynamic impulse.
jeepModelData <- data.frame(Iq=c(),dmin=c(),dmax=c())
Vini <- c(V=0,D=0) #initial conditions of ode
for (Iq in c(.5,.6,.7,.8,1,1.5,2,2.75,4,5,8,10,15,20,27.5,50,80,100)) {
  dmax <- 0
  dmin <- 99999
  print(Iq)
  for (tu_plus in c(.1,.3,.5,.7,.9,1)) {
    F1 <- 8.9029*(.3048/c0)^.61692*tu_plus
```

```
    A <- alpha*p0*1000*tu_plus/c0
    for (r in c(.1,.4,.7,1,3,5)) {
      Qs <- (Iq/p0/tu_plus)/(exp(-r)+r-1)*r^2
      Ps <- find_overpressure(Qs)$root
      for (tp_plus in c(.1,.3,.5,.7,.9,1)) {
        for (n in c(.1,.4,.7,1,3,5)) {
          params <- c(Ps,Qs,n,r,tp_plus/tu_plus,M,RBar,Dlim,Amin,A,Achange,F1,
              g)
          out <- ode(y = Vini, func = objectVelocityWithDecelFletcherFinal,
                     times = seq(0,10,.002), parms = params, method="ode23")
          dmin <- min(dmin,max(out[,3]*tu_plus*c0))
          dmax <- max(dmax,max(out[,3]*tu_plus*c0))
        }
      }
    }
  }
  jeepModelData <- rbind(jeepModelData,data.frame(Iq=Iq,dmin=dmin,dmax=dmax))
}

#Plot simulation prediction against validation data
ggplot(data=jeepModelData) +
  geom_ribbon(aes(Iq,dmin,ymin=dmin,ymax=dmax),alpha=.5) +
  geom_point(data=jeepData,aes(x*6.89476,Curve1*.3048),color="red") +
  scale_x_log10(breaks=c(1,10,100),limits=c(.5,100)) +
  scale_y_log10(breaks=c(1,10,100,1000)) +
  xlab("Dynamic Pressure Impulse (kPa s)") +
  ylab("Displacement (m)") +
  theme_bw() +
  theme(panel.grid.major=element_line(color="gray"),
        panel.grid.minor=element_blank())
ggsave("Figures/jeepDataValidation_v7.pdf",width=4.5,height=4.5)

#write.csv(modelData,"jeepValidationData.csv")
#jeepModelData <- read.csv("jeepValidationData.csv")
```

A.2 Bowen 1961 Translation Model

The following R function is used to calculate an object's maximum velocity based on the model given in Bowen et al. 1961. This function is called using an ODE solver.

```
objectVelocityBowen <- function(Z, y, p) {
  'Function calculates the distance and velocity derivatives for running the
     translation model (called with an ODE solver).  Based on the Bowen 1961
     translation model.
  Inputs:
    Ps - peak overpressure (dimensionless)
    A - acceleration coefficient (dimensionless)
  '
  #State variables
  V <- y[1]
  D <- y[2]

  #Parameters
  Ps <- p[1]
  A <- p[2]

  if (Ps < 0.6) {
    J <- 1.186*Ps^(1/3)
  } else if (Ps <= 1) {
    J <- 1
  } else {
    J <- 10^4*Ps^(-1/4)/(10^4 + Ps^2)
  }
  K <- 1-J
  gamma <- 1/4 + 3.6*Ps^(1/2)
  delta <- 7 + 8*Ps^(1/2) + 2*Ps^2/(240 + Ps)
  Qs <- 2.5*Ps^2/(7+Ps)*(1+2*10^(-8)*Ps^4)/(1+10^(-8)*Ps^4)
  Us <- Ps/(1+Ps^(1/2))
  Xdot_Max <- 3/5*Us + (1+(3/5*Us)^2)^(1/2)
  nu <- Ps^(1/3)+.0032*Ps^(3/2)

  U <- Us*(1-(Xdot_Max*Z-D)/Xdot_Max)*exp(-nu*(Xdot_Max*Z-D)/Xdot_Max)
  #U <- Us*(1-Z)*exp(-nu*Z)
  if (V>=U) {
    return(list(c(V=0,D=0,Zprime=0)))
  } else {
    Q <- Qs*(1-(Xdot_Max*Z-D)/Xdot_Max)*(J*exp(-gamma*(Xdot_Max*Z-D)/Xdot_Max)
        +K*exp(-delta*(Xdot_Max*Z-D)/Xdot_Max))
    #Q <- Qs*(1-Z)*(J*exp(-gamma*Z)+K*exp(-delta*Z))
    dV <- Q*A*((U-V)/U)^2
    dD <- V
    return(list(c(V=dV,D=dD)))
  }
}
```

A.3 Fletcher 1966/1975 Translation Model

The following R function is used to calculate an object's velocity and distance traveled based on both acceleration due to the blast wave and deceleration. This function is called using an ODE solver.

```
objectVelocityWithDecelFletcherFinal <- function(Z, y, p) {
  'Function calculates the distance and velocity derivatives for running the
     translation model (called with an ODE solver).
    Based on Fletcher 1966/1975'

  #State variables
  V <- y[1]
  D <- y[2]

  #Parameters
  Ps <- p[1]
  Qs <- p[2]
  n <- p[3]
  r <- p[4]
  tratio <- p[5]
  M <- p[6]
  RBar <- p[7]
  Dlim <- p[8]
  Amin <- p[9]
  Amax <- p[10]
  Achange <- p[11]
  F1 <- p[12]
  g <- p[13]

  #Acceleration coefficient
  if (D<Dlim){
    A <- Amin+Achange*D^2
  } else {
    A <- Amax
  }

  #Pressure calcuation
  Q=Qs*(1-Z)*exp(-r*Z)
  P=Ps*(1-Z/tratio)*exp(-n*Z/tratio)
  if (Q<0) Q=0
  if (P<0) P=0

  #Calculating wind velocity within shock wave using adiabatic conditions
  Ts <- (7+Ps)/(7+6*Ps)*(1+Ps) #Using RH relation
  TBar <- Ts*((P+1)/(Ps+1))^((g-1)/g)
  RhoBar <- (P+1)/TBar #RhoBar = rho * RT0/P0
  U <- sqrt(2*Q*RBar/RhoBar)
  if (is.na(U)) U=0

  #Return changes to velocity and distance traveled
  if (V<0) {
    return(list(c(0,0)))
  } else if (V>=U) {
```

```
    dV <- -1*F1*(V*(1/M)^(1/6))^0.38308
    dD <- V
  } else {
    dV <- Q*A*((U-V)/U)^2 - F1*(V*(1/M)^(1/6))^0.38308
    dD <- V
  }
  return(list(c(dV,dD)))
}
```

Abbreviations, Acronyms, and Symbols

AIS	abbreviated injury scale
AmedP-8	Allied Medical Publication 8
ARA	Applied Research Associates, Inc.
CI	combat ineffectiveness
DT	decelerative tumbling
DTRA	Defense Threat Reduction Agency
EM-1 Ch. 14	Effects Manual-1 Chapter 14
FI	fatal injury
FME	flexible modeling environment for modeling, sensitivity, and Monte Carlo analysis (R plug-in)
HENRE	Health Effects from Nuclear and Radiation Environments
HPAC	Hazard Prediction and Assessment Capability
HRP	Human Response Panel
IPI	immediate permanent ineffectiveness
ISS	Injury Severity Score
LFMER	Lovelace Foundation for Medical Education and Research
SS	Severities Sum
MHGP	Multi-Hit Glass Penetration
MI	moderate injury
NATO	North Atlantic Treaty Organization
ORCA	Operational Requirement-based Casualty Assessment
PDCALC	Probability of Damage Calculator
PI	perpendicular impact
PRCC	Personnel Risk and Casualty Criteria
R	software programming language for statistical computing
SFOM	Shard Fly-Out Model
SI	serious injury

DEPARTMENT OF DEFENSE

DEFENSE THREAT REDUCTION
AGENCY
8725 JOHN J. KINGMAN ROAD
STOP 6201
FORT BELVOIR, VA 22060
ATTN: P. BLAKE

DEFENSE TECHNICAL
INFORMATION CENTER
8725 JOHN J. KINGMAN ROAD,
SUITE 0944
FT. BELVOIR, VA 22060-6201
ATTN: DTIC/OCA

DEPARTMENT OF DEFENSE CONTRACTORS

QUANTERION SOLUTIONS, INC.
1680 TEXAS STREET, SE
KIRTLAND AFB, NM 87117-5669
ATTN: DTRIAC